NGU REPORT 2018.015

Tomographic Inversion of Synthetic Refraction Seismic Data Using Various Starting Models in Rayfract® software

GEOLOGY FOR SOCIETY

SINCE 1858

GEOLOGICAL SURVEY OF NORWAY

· NGU ·

NORGES GEOLOGISKE UNDERSØKELSE
- NGU -

REPORT

Geological Survey of Norway
P.O.Box 6315 Torgard
NO-7491 TRONDHEIM
Tel.: 47 73 90 40 00

Report no.: 2018.015

ISSN: 0800-3416 (print)
ISSN: 2387-3515 (online)

Grading: Open

Title:
Tomographic Inversion of Synthetic Refraction Seismic Data Using Various Starting Models in Rayfract® software.

Authors:
Georgios Tassis, Siegfried Rohdewald & Jan Steinar Rønning

Client:
Norwegian Public Roads Administration (NPRA) / NGU

County:

Commune:

Map-sheet name (M=1:250.000)

Map-sheet no. and -name (M=1:50.000)

Deposit name and grid-reference:

Number of pages: 45 **Price (NOK):** 150,-
Map enclosures:

Fieldwork carried out:	**Date of report:**	**Project no.:**	**Person responsible:**
	01.10.2018	329500	Marco Brönner

Summary:
This report continues our work on refraction seismic modeling in Rayfract® and explores new possibilities offered by the software to create reliable starting models for Wave Eikonal Traveltime (WET) inversion. For this purpose, we used two complex models based on traditional interpretations from Knappe tunnel survey i.e. P1-1 (120 m) and P1-6/7 (240 m). The first model contains three vertical fracture zones below a thin overburden and the second involves a pair of fracture zones overlain by a thick overburden basin.

DeltatV is a method for generating starting models that hasn't been investigated by us in the past and ideally, long lines (minimum 500 meters) and dense geophone and shot coverage (receivers every 1 or 2 meters and shots every 3rd or 4th geophone) are required. Our models do not match the minimum length specifications, but we created four synthetic datasets (A to D) that match all four combinations of the above receiver/shot requirements. Our first attempt running DeltatV on these datasets has returned results that are contaminated with strong high-frequency artefacts and no clear indication of the modeled fracture zones. Subsequently, using these results as starting models has yielded equally low-quality WET inversion results. However, S. Rohdewald's processing has shown that expert-level knowledge of Rayfract® can yield much better DeltatV / XTV starting models for all P1-6/7 datasets. DeltatV / XTV could not produce successful starting models for model P1-1, but more elaborate inversion schemes led to better WET inversion results.

In previous reports we have shown that interactive picking of branch points along traveltime curves followed by **Hagedoorn's Plus-Minus** method can generate starting models which are very accurate even for data collected with sparser receiver/shot spacings. Moreover, branch point picking enables the use of **Wavefront** method as an alternative to Plus-Minus while these two methods can also be implemented semi-automatically with the use of **midpoint breaks** option. This is achieved by specifying a combination of parameters which replaces the time-consuming process of mapping traveltimes to refractors. Using all above mentioned options and methods, far better starting models than created by DeltatV were acquired which in turn led to equally successful WET inversion results. **In any case, the combination of branch point picking and Hagedoorn's Plus-Minus method still yields the best outcome.**

Finally, we examined the effect a low-velocity overburden layer can have on the success of WET inversion. We tested 20 and 40-meter overburden layers that follow topography on both models using the least dense receiver/shot point coverage (2/8 meters respectively) with the most successful procedure i.e. with interactive branch point picking and Plus-Minus method. We have concluded that for shorter lines, an overburden layer of 20 m can inhibit fracture zone detection but not entirely while 40 m of low-velocity top layer critically limits resolution in depth. Finally, ray coverage graphs indicate that longer lines with proper distant shots acquired (like P1-6/7) can have higher depth penetration although success is questionable. More far-offset shots and using overlapping receiver spreads may further improve the results.

Keywords:	Geophysics	Fracture zones in bedrock
Detection	Characterization	Refraction seismic
Tomographic inversion	Modelling	Scientific report

CONTENTS

1. INTRODUCTION

This report presents further investigations on how to produce a trustworthy starting model from synthetic refraction seismic data which is essential in obtaining a trustworthy Wave Eikonal Traveltime or WET inversion result (Schuster & Quintus-Bosz 1993) in Rayfract® software (Rayfract 2018a & -b). This is achieved by exploring more options offered by the program for obtaining starting models with more focus given to the DeltatV method (Gebrande & Miller 1985), and XTV method (Rayfract 2018b) which are methods some private contractors use for processing and interpreting refraction seismic data. NGU has already done lots of modeling work on this subject (Rønning et al. 2016; Tassis et al. 2017) based on real refraction data collected prior to the construction of Knappe tunnel west of Bergen. Whether refraction seismic inversion can be used for the detection of fracture zones in bedrock remains the aim of this study. The modeling base for that will be the same traditional interpretation profiles P1-1 and P1-6/7 from Knappe also used in Tassis et al. (2017).

In addition to the use of DeltatV+XTV method and subsequent WET inversion, this report also utilizes experience obtained earlier by the NGU for inverting refraction seismic data i.e. using the interactively picked branch points and the implementation of built-in Hagedoorn's Plus Minus method (Hagedoorn 1959) to calculate an accurate starting model. More starting models are also produced with the use of Wavefront method for picked traveltime branch points, but also by employing both Plus-Minus and Wavefront methods using common midpoint breaks display instead of interactive branch point picking. Therefore, this report demonstrates five different ways for producing five different starting models within Rayfract®, four of which have not been investigated by us in the past.

Figure 1.1.1 shows a flow-chart with all available routes a user can take to arrive at WET inversion result using Rayfract®. The same figure has been introduced in Tassis et al. (2017) but this updated version contains one more bracket for midpoint breaks method i.e. one more tool to produce a starting model. Black arrows show the options that have been employed in this report to obtain an inversion result.

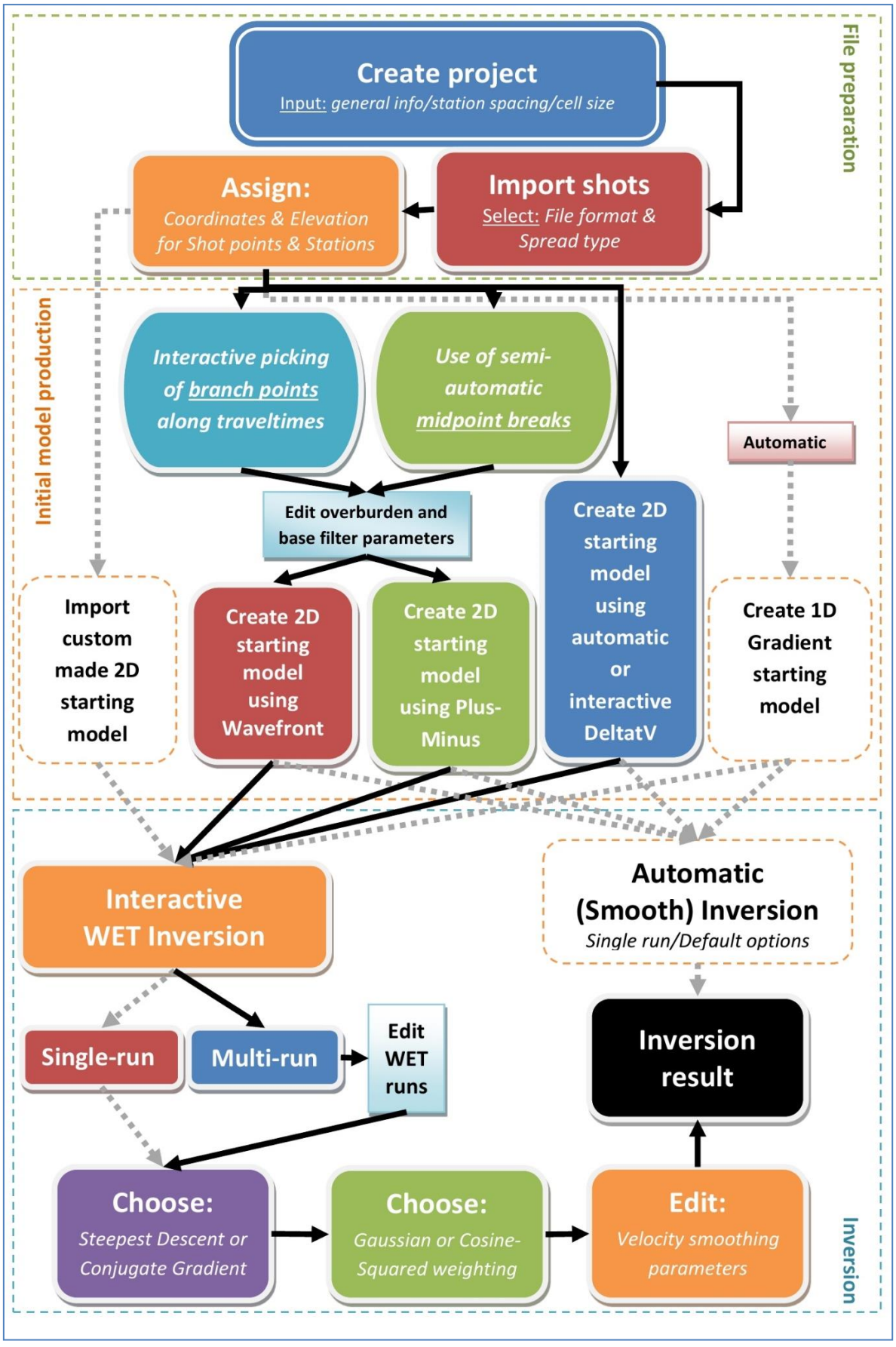

Figure 1.1.1: *Flowchart for Rayfract® software. Black arrows show procedures we have used in this report and gray dotted arrows other options available with the software (most of them utilized in Tassis et al. 2017).*

2. DESCRIPTION OF DELTATV METHOD

DeltatV is a seismic refraction inversion method which inverts refracted traveltimes into a depth-velocity model. It sorts rays by Common MidPoint (CMP) and inverts individual CMP traveltime curves with the layer-stripping method. Unlike Hagedoorn's Plus-Minus method, which has been investigated in previous NGU reports, DeltatV does not require the interactive assignment of traveltimes to hypothetical and mathematically idealized refractors. Sorting traveltimes by common midpoint (CMP) instead of common shot, averages out the effects of dipping layers on traveltimes. The traveltime field is smoothed naturally by stacking CMP-sorted traveltime curves over a few adjacent CMP's. Then each CMP curve is independently inverted with the 1D DeltatV method. It is based on "seismic stripping" of assumed incremental layers with constant vertical velocity gradients and positive or negative velocity steps at layer boundaries. The XTV layer option for DeltatV lets the user specify a velocity contrast level above which the CMP intercept-time method is used instead of diving-wave DeltatV method.

The constant velocity gradient assumption for DeltatV means that seismic rays follow circular arc segments inside each layer modeled (diving waves, see Figure 2.1). Consequently, rays can be reconstructed and treated analytically. The method estimates the layer bottom velocity from traveltimes and then inverts for the layer top velocity by solving a system of two equations numerically. Seismic stripping is equivalent to physically lowering source and receiver for each such ray to the top of the next lower layer. Inversion of these reduced traveltimes and offsets then resolves the properties of this lower layer (Rayfract 2018b). DeltatV method favors a gradient velocity model which is not the best option for areas in Norway where glacial erosion has removed weathered bedrock. Short receiver (1 – 2 m) and shot spacings (3 – 4 times receiver spacing) are required and preferably long lines (> 500 m) recorded using overlapping receiver spreads (Rayfract 2018b).

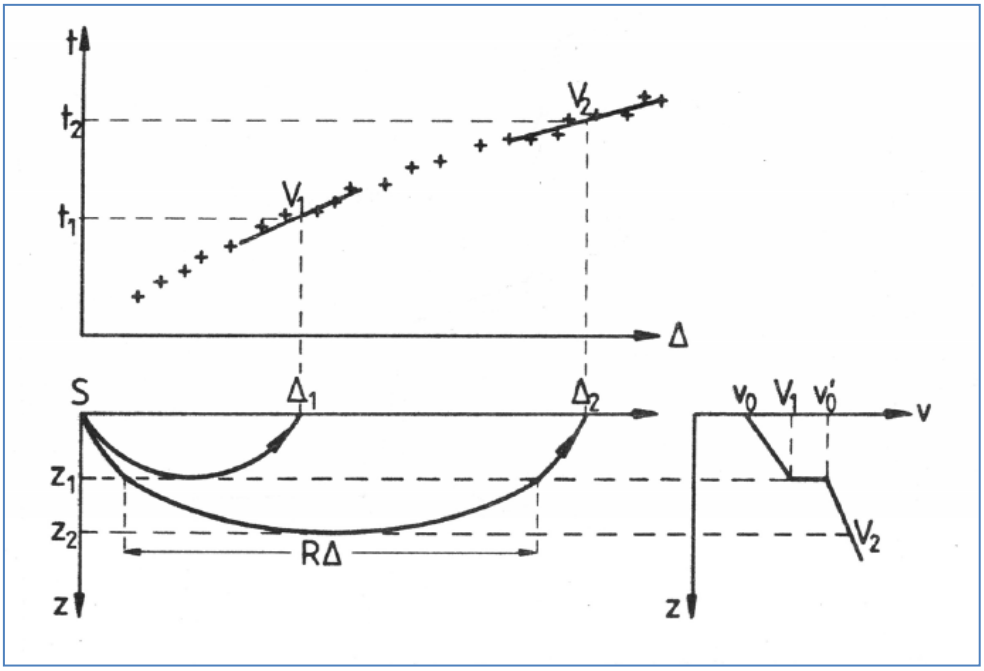

Figure 2.1: Principle of diving waves based on a velocity model with gradient increase of seismic velocities within layers. Note the curvature in the travel time curve (top figure) (after Gebrande & Miller 1985).

3. MODELS & SYNTHETIC DATA

The basis for the modeling effort presented in this report is borrowed from the traditional Plus-Minus interpretations done for profiles P1-1 and P1-6/7 from Knappe tunnel (Wåle 2009). These two models are shown in **figure 3.1.1.** P1-1 presents three subsequent fracture zones (3800 m/s – 15, 10 and 10 m wide respectively) with thin overburden presence while P1-6/7 shows two adjacent fracture zones (3400 and 2800 m/s respectively – 25 m aggregate width) overlain by 10 meters of low-velocity (sediment) formations. These base models were constructed as grids in Surfer 15 (Golden Software 2018) and then imported into Rayfract® for traveltime calculation according to specified shot and receiver spacings (forward modeling, Rayfract 2018b). Synthetic data based on these models were also constructed in the past (Tassis et al. 2017), but the shot and geophone spacing used was 20 and 5 m respectively.

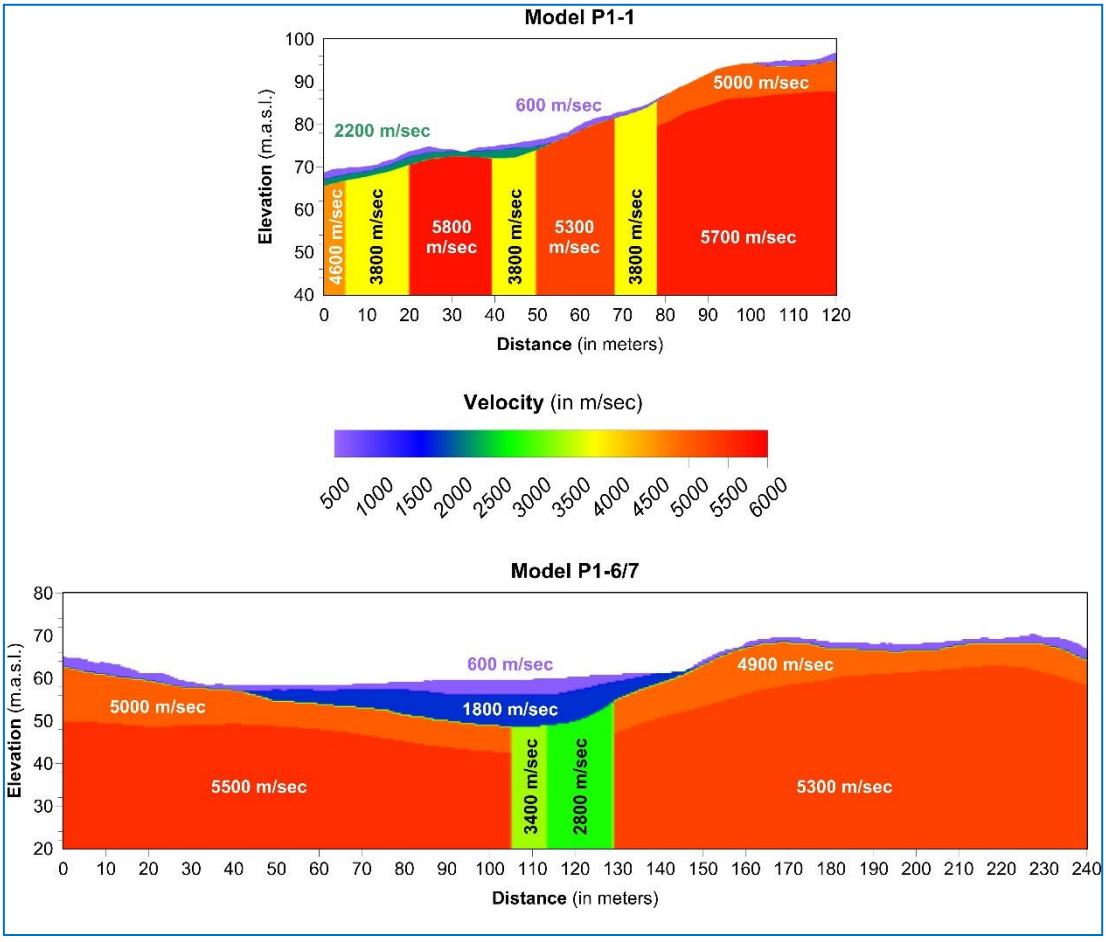

Figure 3.1.1: *Surfer 15 grids based on traditional interpretations done for profiles P1-1 and P1-6/7 from Knappe (Wåle, 2009). Elevation in meters above sea level (m.a.s.l.).*

Theoretically, DeltatV works best with long lines (500 m or longer) recorded using overlapping receiver spreads and roll-along method used in reflection seismics and with dense shot and receiver spacing. Therefore, modeled line lengths equal to 120 and 240 m used in this report are not ideal for DeltatV. The construction of a 500 m long model would be extremely time consuming and not as detailed due to Rayfract® grid point number limitations. However, for models such as the ones tested here, using a receiver spacing of 1 m or maximally 2 m and a shot at every 3rd or 4th receiver is

proposed (ten or more shots per line required). Also, offset shots positioned to left of first receiver/to right of last receiver can be utilized to improve the performance of DeltatV method. Essentially, new models with high geophone and shot point density were constructed for this modeling procedure since the old synthetic data based on the same traditional Plus-Minus cross-sections, employed a configuration unsuitable for DeltatV application.

Four versions of synthetic data have been compiled for each model:

- Dataset A using 1 m receiver and 3 m shot spacing,
- Dataset B using 1 m receiver and 4 m shot spacing,
- Dataset C using 2 m receiver and 6 m shot spacing,
- Dataset D using 2 m receiver and 8 m shot spacing.

Figure 3.1.2 displays the synthetic traveltimes compiled by Rayfract® for dataset P1-1A and **figure 3.1.3** the synthetic traveltimes for dataset P1-6/7A. All receiver and shot points have the same coordinates as the data from Knappe and elevation from detailed LiDAR topography. Generally, modelled traveltime curves show a lot of systematic / parallel "oscillation". This is likely caused by the extreme topography variation along the profile. It would probably help to apply a running average smoothing filter to the model's topography (z coordinate) along the x axis, before forward-modelling the synthetic shots, but this would be an attempt to hide real topographic challenges.

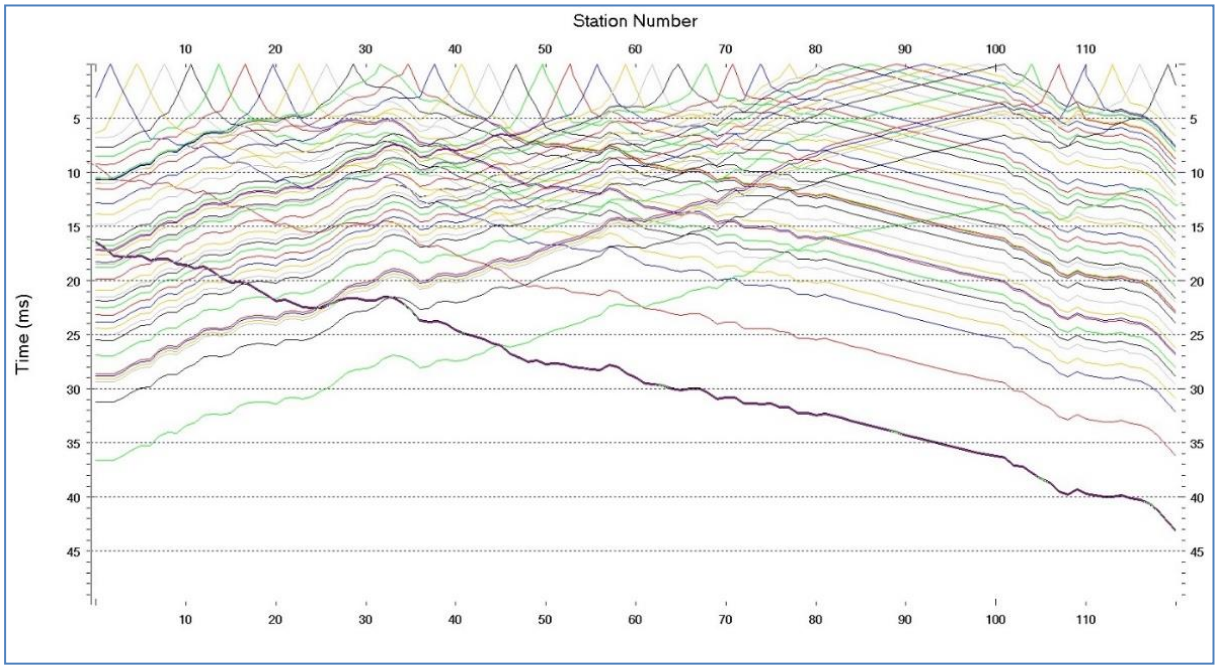

Figure 3.1.2: *Synthetic traveltimes compiled by Rayfract® for dataset P1-1A (receiver spacing 1 m, shot spacing 3 m).*

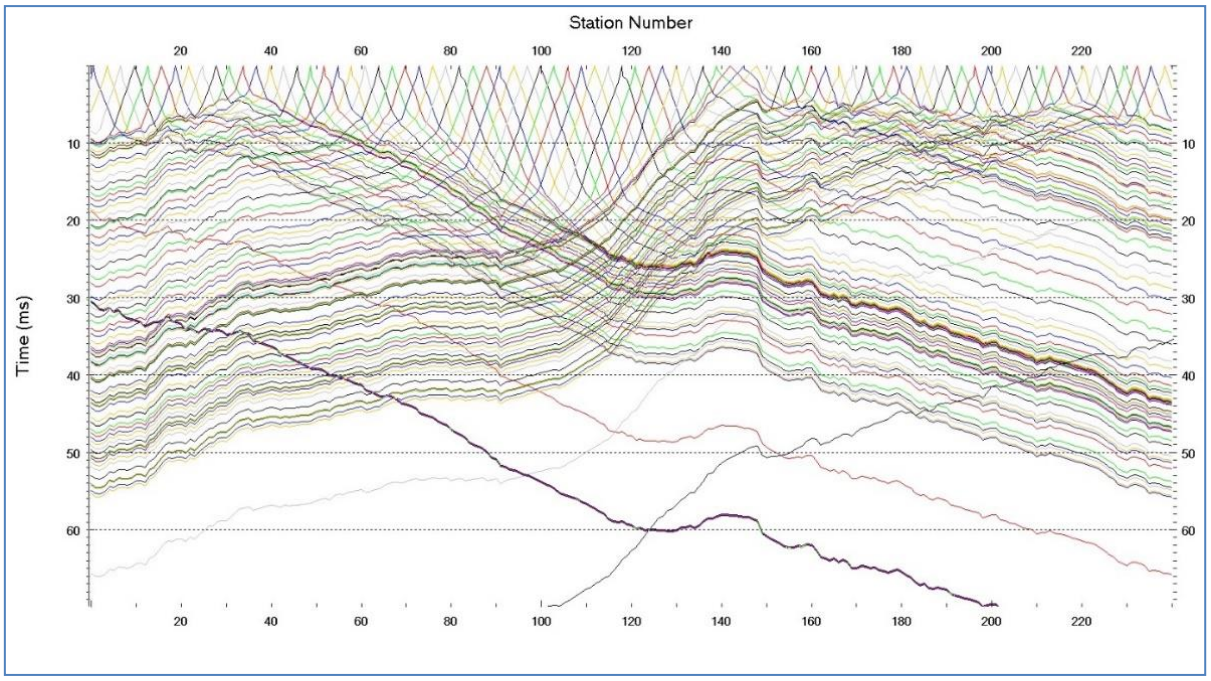

Figure 3.1.3: *Synthetic traveltimes compiled by Rayfract® for dataset P1-6/7A (receiver spacing 1 m, shot spacing 3 m).*

4. DELTATV METHOD APPLICATION

When working with DeltatV application, most weight should be given to near surface imaging. The deeper the structure imaged, the more uncertainty is involved in determining depth and velocity. This is caused by accumulation of modeling errors in the overburden, during reduction of deeper traveltimes to the next lower level (overburden layer stripping). Considering this and before the actual application of DeltatV inversion, a theoretical examination of the models must be made to set the bar for expectations. For model P1-1 with three vertical low-velocity fault zones, DeltatV is not expected to function too well due to related artefacts in case of strong refractor curvature. Furthermore, for model P1-6/7 with overburden layer over a fractured zone, our expectations should also be low since DeltatV has issues with resolving a sudden increase of velocity with depth. But XTV layer option helps with imaging strong velocity contrast between layers (Rayfract 2018b). Finally, a warning message is given when DeltatV is initiated within the program indicating that "*Pseudo-2D DeltatV inversion will result in velocity artefacts, in case of strong lateral velocity variation*" which is the case in this modeling effort. In addition, strong lateral velocity variation also includes strongly undulating topography which is common in Norwegian landscapes. More specifically, DeltatV produces systematic artefacts in case of strong basement refractor or topography curvatures - too low velocity below anticlines and too high velocity below synclines. This is not a flaw of the software but instead is caused by the CMP sorted ray geometry.

DeltatV does not really compete with WET inversion, especially when vertical structures such as fracture zones are apparent. Rather, DeltatV is an alternative method for determining a starting model, instead of using layered refraction methods such as Plus-Minus or Wavefront. Regardless, since the compilation of an accurate

starting model is of the utmost importance for the success of any WET inversion, we will investigate the quality of starting models DeltatV and DeltatV +XTV can provide.

4.1 Dataset P1-1A starting models

All presented DeltatV result utilized the “Interactive DeltatV (CMP velocity versus Depth)” option in Rayfract®. Since there is no simple rule regarding which DeltatV settings best allow imaging of vertical structures, we have tested a series of parameter combinations to empirically discern whether fracture zones can be detected by the method. **Figure 4.1.1** shows a series of obtained results for dataset P1-1A varying from default to more sophisticated.

Implementation of interactive DeltatV starting model generations is semi-automatic and does not require the user to specify crossover points. The user is presented with two sets of parameters to tune: a set for generic DeltatV and another for static first break corrections. However, it is required to first obtain smoother starting models with less noise/artefacts with non-default DeltatV settings. The reason for that is that Pseudo 2D DeltatV application is characterized by imaging artefacts when strong lateral velocity variations are apparent (as in our case) but additionally caused by Golden Software Surfer Kriging gridding method. As can be seen in the bottom left of **figure 4.1.1**, checking options *Suppress Velocity Artefacts* and *Smooth CMP Traveltime Curves* limits artefacts, even though the result is not very close to the synthetic model seen at the top left. Finally, parameter *Maximum valid velocity* lets you specify the maximum apparent velocity value accepted as valid when processing CMP curves and since it is known, it was set equal to 6000 m/s. Apparent CMP velocities higher than this value have been skipped. Increasing *Maximum valid velocity* to 8000 m/s can help to avoid DeltatV artefacts.

Moving away from standard DeltatV parameters, two of them stand out from the generic set: *CMP curves stack width* (referred to as CMPs in figures) and *Regression over offset stations* (referred to as Regression) which allow the user to specify to what degree the traveltime data is smoothed horizontally and vertically. It is advised to vary parameter *Regression over offset stations* between values of 5 to 20. Generally, smaller values for this parameter will deliver shallower depths for the same velocity. For low-coverage surveys or situations of high velocity contrasts between clearly recognizable layers, it is recommended setting this parameter to a value near the minimum value of 5. The minimum allowed value is 3. Also, the suggested variation width for parameter CMP curves stack should be between 10 to 50. Following these recommendations and aiming at highlighting vertical structures, we found that CMP curves stack width equal to 15 and Regression over offset stations equal to 5 return the results with a higher lateral variation in velocities (right hand side of **figure 4.1.1**). Increasing *Static correction parameter Inverse CMP Offset power* from default 0.5 to 0.9 also increases the lateral resolution of DeltatV velocity (P1-1). Decreasing Inverse CMP Offset Power to 0.1 or 0.2 results in more laterally smoothed DeltatV velocity (P1-6/7A) within each CMP curve stack.

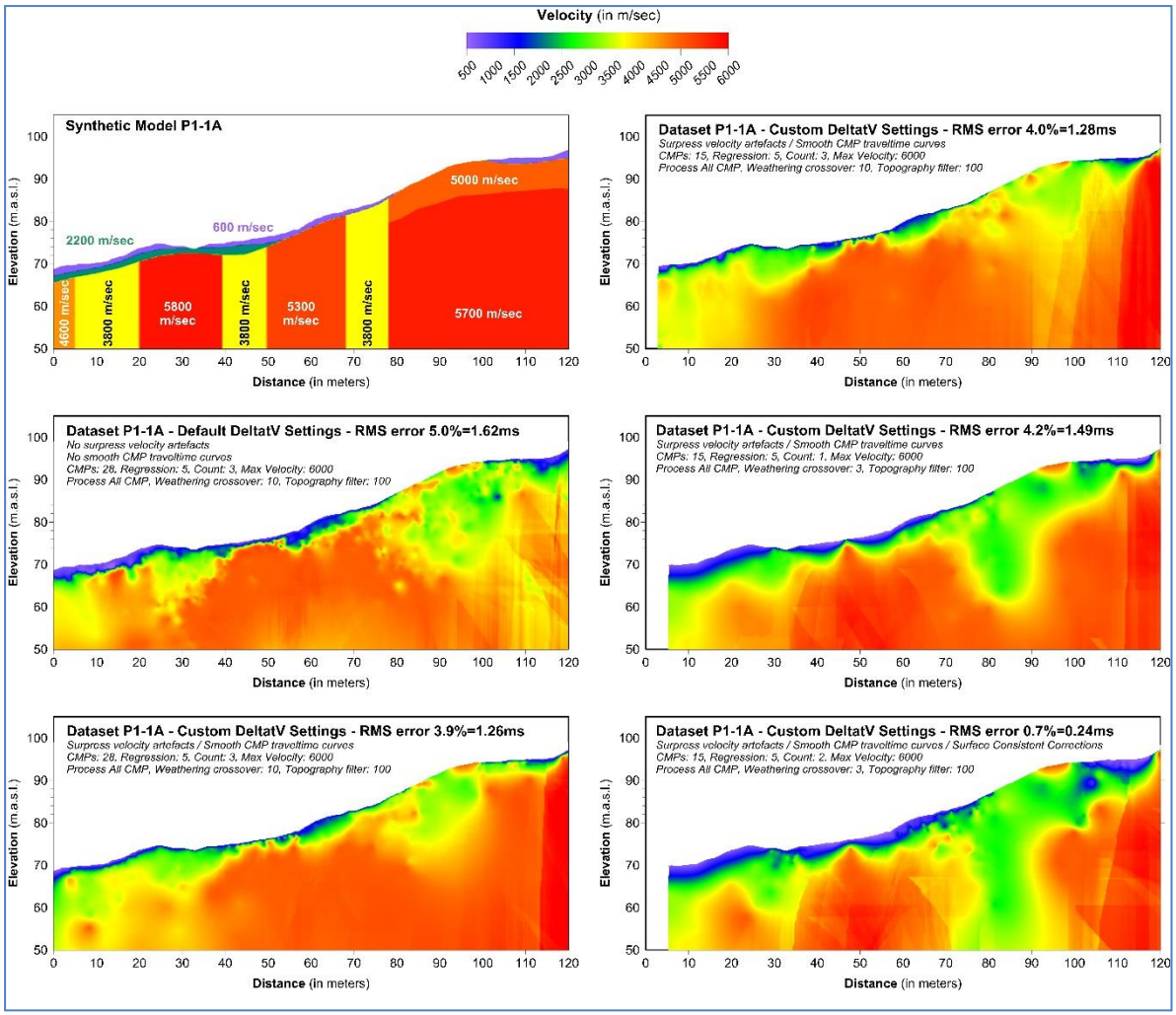

Figure 4.1.1: *Interactive DeltatV (CMP velocity versus Depth) calculations on dataset P1-1A with a variety of utilized parameters listed with each profile. All profiles constitute possible starting models to be used by WET inversion.*

By decreasing the value of *Weathering sub-layer count* (referred to as Count) to 1 and then to 2 (middle right and bottom right part of **figure 4.1.1** - default value: 3), we obtained less detailed topmost / weathering velocity imaging and higher fragmentation degree within “bedrock”. Combining this with the decrease of parameter *Weathering crossover* to 3 (default value: 10), which specifies the estimated average crossover distance separating direct wave arrivals from refracted arrivals, we have caused a higher lateral variation in velocity in our inversion results. Finally, checking the static first break correction option *Surface Consistent Correction* we have managed to push the relative RMS error to drop to 0.7 % (0.24 ms), which is way smaller than the errors obtained for the other two results shown at the right-hand side of **figure 4.1.1** (4.0 and 4.2 %).

Unfortunately, DeltatV results for dataset P1-1A are not very promising. One could interpret three fracture zones in the result: one around the beginning of the profile, a second between 25 and 35 meters and a last one between 70 and 90 meters. However, these zones do not match the modeled ones neither in positioning, width nor calculated velocity. If we assume that the low-velocity concentrations seen at the beginning and end of the profile are due to the respective modeled zones, it is safe to conclude that the middle zone is not detectable by DeltatV. All the same, we cannot conceive these

“detected” zones as a success for the method since their velocities are much lower than the modeled ones (about 1000 m/s difference), they are misplaced i.e. appearing with a 10-meter offset and their width is either not easily discernable or bigger than modeled. Moreover, the use of non-default DeltatV setting has caused a higher lateral variation within “bedrock” but also created an equally low-velocity horizontal layer just below the thin modeled overburden. Especially near the end of the profile, this additional overburden is very much pronounced, and this is probably due to the differentiation in modeled bedrock velocity with depth (5000 m/s top – 5700 m/s bottom). When we use one of these DeltatV results as a starting model, there is a risk that these local minima can disturb inversion in a way that the algorithm will put more weight on matching these high velocity contrasts at the expense of other areas. In any case, the DeltatV result shown at the bottom right of **figure 4.1.1** is considered to be better approximating the synthetic model but not well enough on any account.

Regardless of the little overall success that DeltatV implementation has achieved in the context of fracture zone detection, it should be noted that there are also some positive points about it. More specifically, the calculation of the top low-velocity layer is quite accurate, even with the use of default DeltatV options and without any interactive picking of branch points. The calculated velocity of the overburden is close to the modeled one and the method can differentiate two layers even though the velocity for the bottom overburden layer is underestimated. Moreover, the overall bedrock velocity is not that far off, especially with higher *Weathering sub-layer count* values (3 or more). Finally, these results were obtained in a matter of seconds, even with the use of the more time-consuming - according to the program developer - *Least Squares* linear regression method as opposed to the faster *Least Deviations* alternative.

4.2 P1-1 WET inversion with DeltatV starting models

Dataset P1-1A presents the densest receiver and shot point positioning but additional synthetic datasets P1-1B, -C and -D have also been compiled using sparser receiver and shot points. This is expected to result in generally poorer results but DeltatV application was applied on these datasets nonetheless using the same parameters as in dataset P1-1A (see bottom right in **figure 4.1.1**). The DeltatV generated starting model results obtained are shown on the left hand side of **figure 4.2.1** while the right hand side displays the WET inversion outcomes using the aforementioned DeltatV starting models for each dataset. WET inversion was implemented by utilizing *Conjugate Gradient inversion, Cosine-Squared weighting, 9 WET runs (iterations), 50 Hz frequency, multirun WET with wavepath width from 30 to 21 %* and *minimal smoothing* as previously found to be the best inversion procedure (Tassis et al. 2017). More information about these parameters and the logic behind choosing them can be found in Tassis et al. (2017).

Figure 4.2.1 validates the assumption that less dense receiver and/or shot spacing datasets has deteriorating effects in DeltatV output. The results for synthetic dataset P1-1A which is the densest in both receiver and shot spacing were already not optimal so the quality of DeltatV output drops even further as receiver and/or shot spacing becomes sparser. Looking at the left-hand side of **figure 4.2.1** we may deduce that possible interpretable fracture zones that match the modeled ones are becoming fewer and fewer with more sparse datasets. Synthetic dataset P1-1B which has equal receiver spacing with P1-1A but slightly sparser shot spacing (4 m instead of 3 m),

presents an image similar to P1-1A but also a clear artefact near its end that could be misinterpreted as a weak zone. Both datasets P1-1C and -D which have sparser receiver spacing (2 m) and even sparser shot point spacing (6 and 8 m respectively) compared to A and B, only present a strong low-velocity concentration at the beginning of each profile but fail to outline any of the other two modeled zones. One interesting feature in DeltatV output for dataset P1-1D is the low-velocity concentration between 50 and 60 m that matches the modeled zone in the middle of model P1-1. However, this feature can only be interpreted as an artefact since its shape is formulated by two hyperbolic high-velocity concentrations. This shows how DeltatV application artefacts can lead to misinterpretations.

The right-hand side of **figure 4.2.1** examines whether DeltatV results could be used as starting models for WET inversion. Generally, the quality of the starting model is of great importance to the success of WET inversion. It has been shown in Tassis et al. (2017) that the application of Plus-Minus method on the same subsurface model can yield very successful outcomes for receiver and shot spacing equal to 5 and 30 meters respectively. For model P1-1 all zones have been detectable from the Plus-Minus stage and WET inversion only had to improve their quantitative characteristics. In this sense, DeltatV output already presents difficulties for WET inversion to resolve and low-velocity artefacts that could interfere with inversion itself.

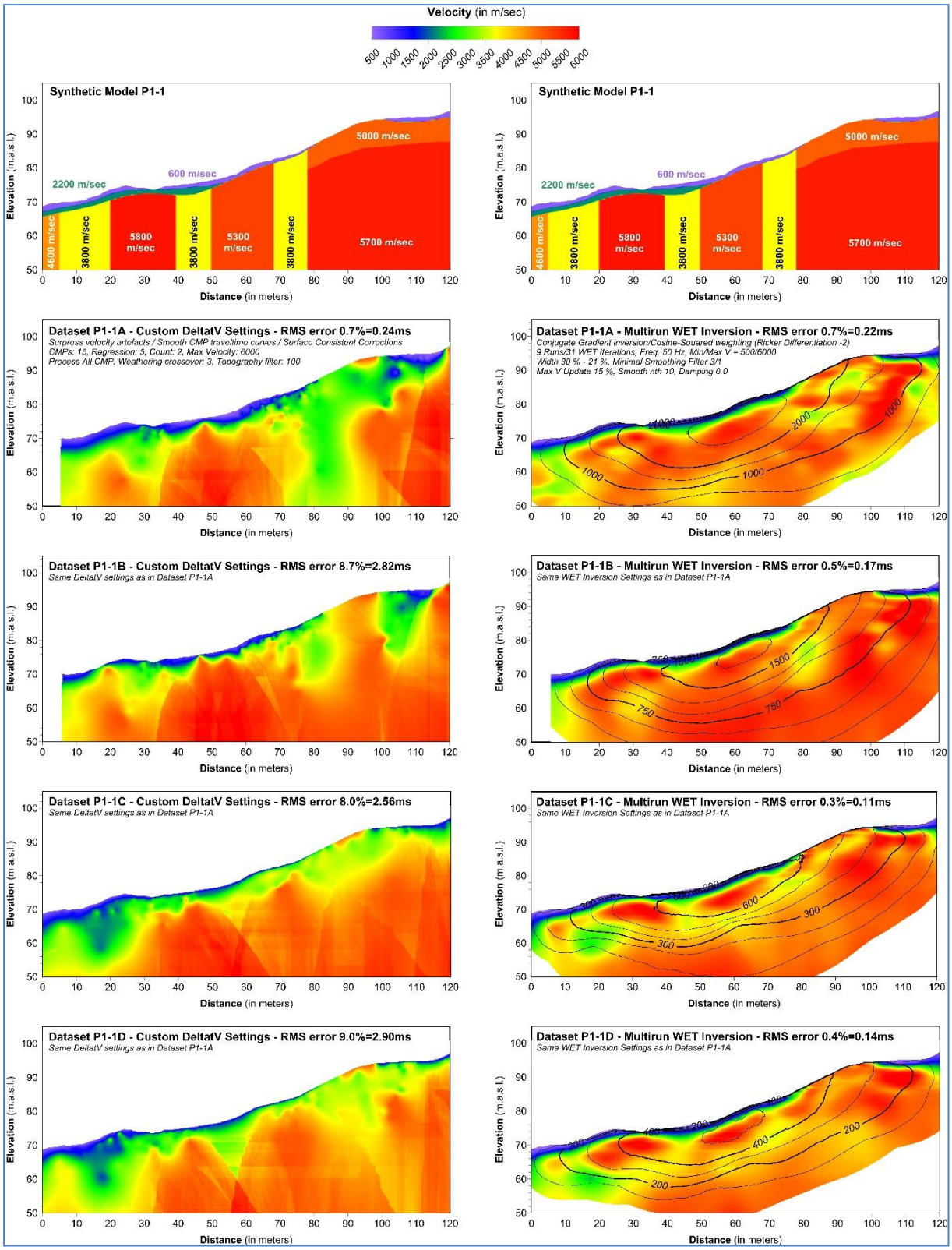

Figure 4.2.1: *DeltatV application results for synthetic data P1-1A, -B, -C and -D obtained from model P1-1 shown on top. Left: starting models using the same DeltatV parameters. Right: Multirun WET inversion results using the DeltatV starting models. Contours represent the ray coverage for each WET tomogram.*

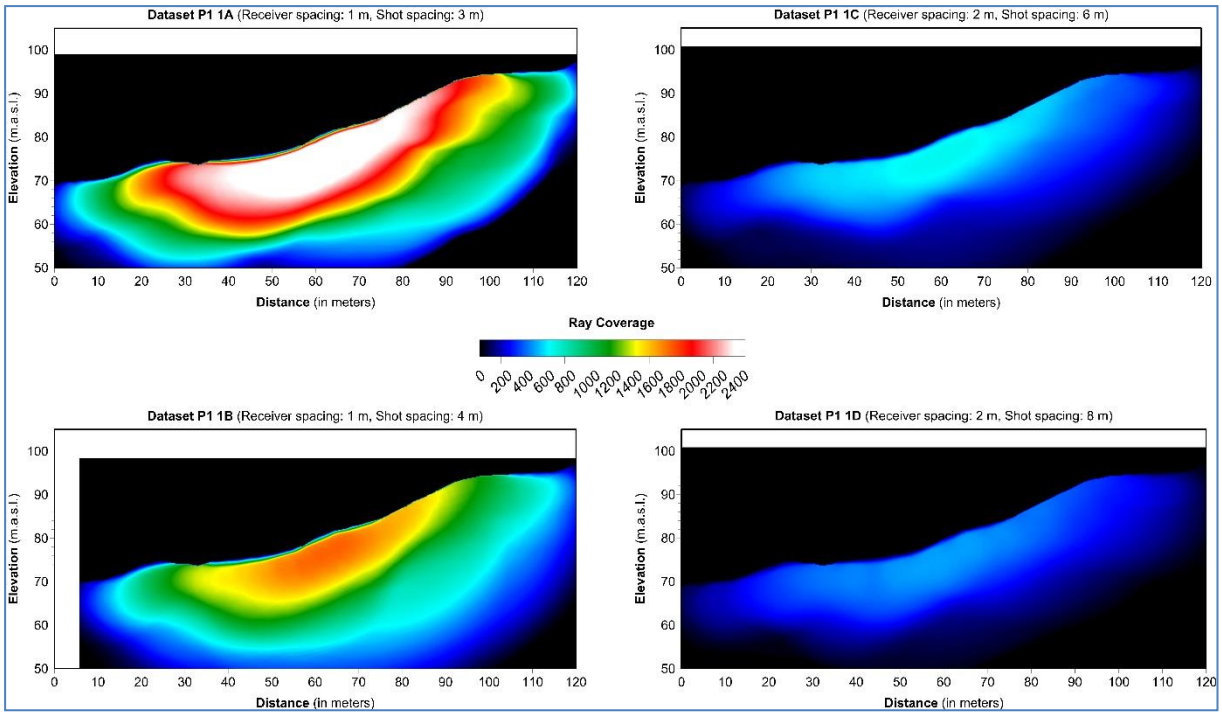

Figure 4.2.2: *Wavepath (ray) coverage graphs for WET tomograms of synthetic data P1-1A (top left), B (bottom left), C (top right) and D (bottom right) using a common color scale.*

WET inversion using DeltatV results as starting models the way we first tested, does not return very promising results. For datasets P1-1A and -B (densest receiver spacing), WET inversion has only led to hints of the modeled zones and no clear indication of their presence. The same observation can be made for datasets P1-1C and -D (less dense receiver spacing) where the overall velocity environment has dropped and whatever indications there are about zones were lost inside a mid-velocity layer parallel to the surface. Furthermore, as can be seen both on the right-hand side of **figure 4.2.1** and separately on **figure 4.2.2** wavepath (ray) coverage is decreasing therefore making results less trustworthy and dubious.

4.3 Dataset P1-6/7A starting models

The same DeltatV parameter investigation shown in chapter 4.1 is repeated here for dataset P1-6/7A which was compiled with the densest receiver/shot spacing out of all the datasets based on Model P1-6/7 (seen in bottom **figure 3.1.1).** Model P1-6/7 is twice as long as model P1-1 (240 m instead of 120) and closer to the shortest recommended profile length for DeltatV application (500 m). It is interesting to see how DeltatV works with longer lines and in this case a simpler model.

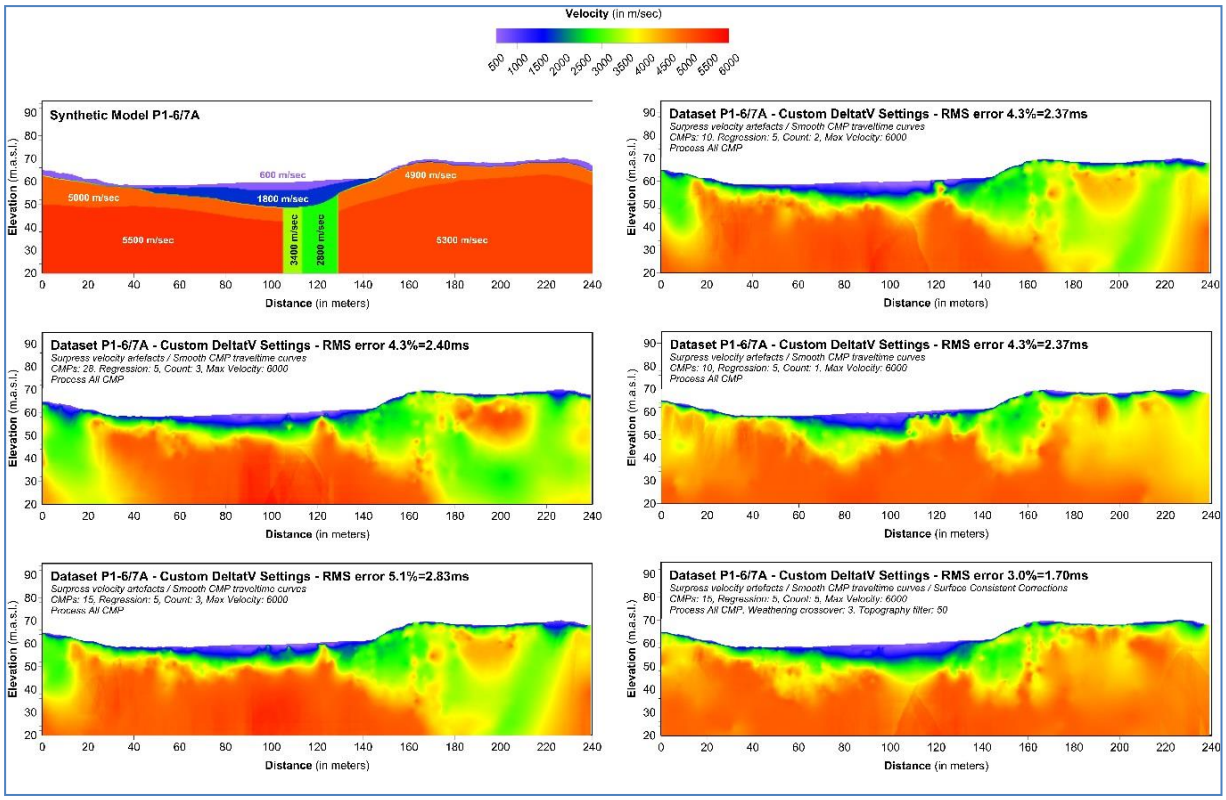

Figure 4.3.1: *Interactive DeltatV (CMP velocity versus Depth) starting model calculations on dataset P1-6/7A with a variety of utilized parameters listed with each profile.*

Figure 4.3.1 presents the DeltatV generation of starting models on dataset P1-6/7A using various parameters. What is easily seen here, at our first attempt to generate starting models, is that there are many artificial effects on both ends of the profile and/or the low-velocity basin in the middle of model P1-6/7, but especially on the second half of the profile. The low-velocity overburden is mapped relatively well but the thick top bedrock layer (4800 m/s weathered rock) is replaced by an equivalent thinner but with lower velocity (2800 m/s) layer instead. Decreasing of *CMP curves stack width* to 15 (bottom left) and then to 10 (top right) seems to have little effect on suppressing the aforementioned artefacts. Parameter *Regression over offset stations* is kept constant to 5 as suggested but decreasing *Weathering sub-layer count* from 3 to 2 (top right) and subsequently to 1 (middle right) which had a positive effect on dataset P1-1A, was an equally beneficial factor on P1-6/7A. This change has diminished artefacts at the edges of the profile but at the same time deteriorated the shape of the basin. Finally. the best overall result was achieved when *Weathering Crossover* was decreased to 3 (default value 10) and when *Topography filter* was reduced to 50 (default value 100). This result can be seen at the bottom right side of **figure 4.3.1** and presents the fewest artefacts, the best basin formulation and the only vague hint of a fracture zone beneath the basin out of all DeltatV generated starting models. However, regardless of the good overall results and the low RMS error (3 %), DeltatV fails altogether in successfully detecting the very pronounced pair of modeled fracture zones beneath the basin.

4.4 P1-6/7 WET inversion with DeltatV starting models

Left-hand side in **figure 4.4.1** displays the result of the first attempt of DeltatV application using the assumed best parameter combination on synthetic datasets P1-6/7A -B, -C and -D. The right-hand side shows the outcome of applying WET inversion using the starting model to the left with the same WET parameters as in **section 4.2**. Both sets of inversion results are presented in alignment with synthetic model P1-6/7 (shown on top of both results) to help make observations concerning the level of success for each method.

As expected, running DeltatV on the remaining synthetic datasets P1-6/7B, -C and -D produced results that were inferior to the result for dataset P1-6/7A. This is also reflected on the RMS error which increases gradually with each dataset from 3 % to 6.5 %. As receiver/shot spacing becomes sparser, so do the low-velocity artefacts whereas the shape of the modeled basin is interrupted by a local high-velocity concentration around its center. Needless to mention that the pair of modeled fracture zones beneath the basin remain undetected in all results.

Looking at the WET inversion results using DeltatV generated starting models on the right-hand side of **figure 4.4.1**, we immediately see that the pair of modeled fracture zones in model P1-6/7 remain undetected. However, the shape of the basin, its internal velocity structure and the rest of the low-velocity overburden are almost flawless. The overall velocity regime for bedrock is of course underestimated in all cases but when denser receiver/shot points are used, it is closer to its modeled values. All results present lower RMS errors than DeltatV starting model while WET inversion has suppressed most of the artefacts seen in the starting models. It could be said that all datasets give a hint of a fracture zone around 120 meters, but without the knowledge of the true model it is difficult to place a possible fracture zone in that position. Finally, WET inversion as it is performed here cannot resolve the abrupt change in velocity from overburden to bedrock and follows the pattern given by the DeltatV starting models i.e. calculates a relatively thin low-velocity layer (~2800 m/s) at the place of the thicker modeled overburden (4800 m/s).

Right-hand side of **figure 4.4.1** and all plots in **figure 4.4.2** show high wavepath (ray) coverage for all four synthetic datasets (as contours in Figure 4.4.1) which gives more trusted inversion results when such dense receiver/shot spacing is used. Dataset P1-6/7A WET inversion result has its most trustworthy middle part starting from 3,000 rays up to 10,000 whereas the highest ray coverage in the same space for Dataset P1-6/7D is starting from 600 and goes up to 2,000 rays. However, the benefit of high receiver and shot point density cannot be shown here due to the use of DeltatV starting models but will be highlighted in the following section of this report.

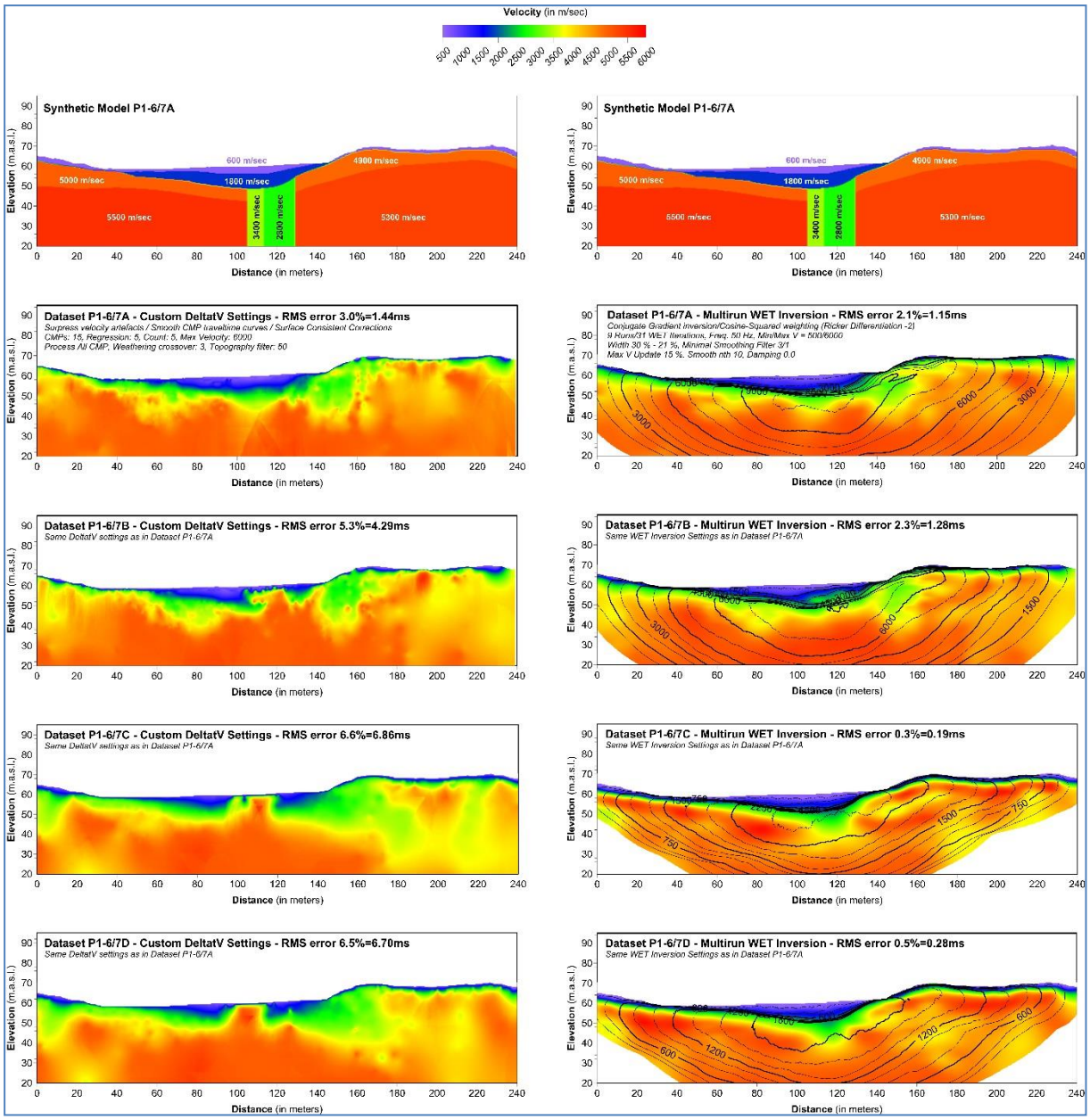

Figure 4.4.1: *DeltatV application results for synthetic data P1-6/7A, -B, -C and -D obtained by model P1-6/7 shown on top using the same DeltatV parameters (Left). Multirun WET inversion results using the DeltatV results shown in the left as starting models. Contours represent ray coverage for each WET inversion result (Right).*

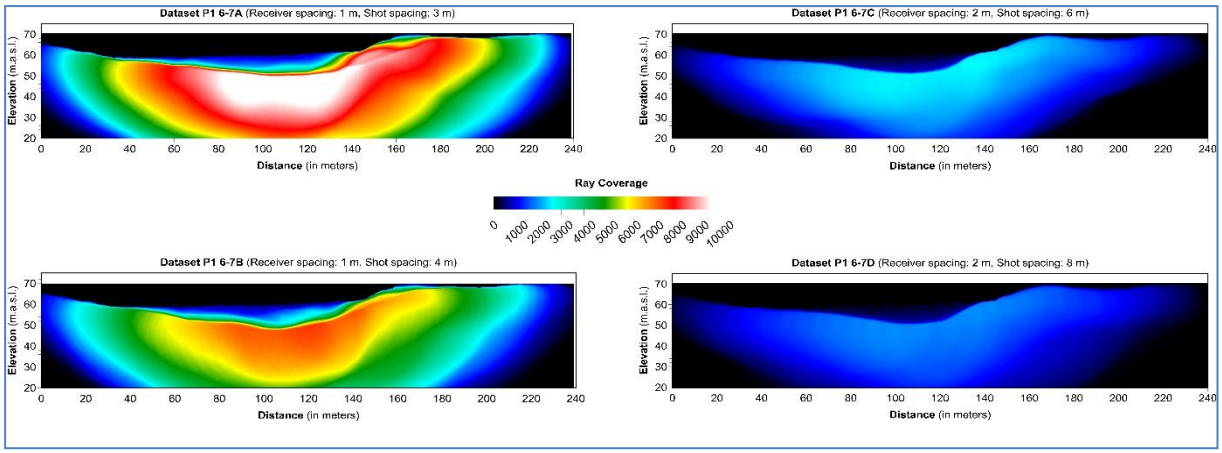

Figure 4.4.2: *Wavepath (ray) coverage graphs for WET inversion results of synthetic data P1-6/7A (top left), B (bottom left), C (top right) and D (bottom right) using a common color scale.*

4.5 DeltatV / XTV enabled application by Rayfract®

During the compilation of this report and in connection with the poor DeltatV results we had obtained, we shared our synthetic datasets with Rayfract® developer S. Rohdewald. He in turn provided us with insightful comments and results of his own to point out that some of the DeltatV starting models and their subsequent inversions could be improved. This was achieved by enabling XTV layered option and by fine-tuning the DeltatV parameters. XTV combines CMP intercept-time method with DeltatV method and allows for Dix inversion considering reflected rays while S. Rohdewald's perfect knowledge of the software led to the compilation of more effective DeltatV parameter sets. Moreover, the gridding method for DeltatV results can also play a role in how representative the final model output will be. Imaging artefacts can be caused solely by Golden Software Surfer Kriging gridding method in some cases. Thus, *Natural Neighbor gridding method* was used in some cases since it can work better for imaging of pseudo-2D XTV inversion output.

Figure 4.5.1 displays the results created by S. Rohdewald. Left side shows calculated *DeltatV / XTV* starting models and right side the respective WET inversion results for P1-1 using the aforementioned starting models. The parameters used for each *DeltatV / XTV* and WET inversion implementation are shown in each profile. Concerning DeltatV, the main differences between our approach and S. Rohdewald's, is using layered XTV option, much lower *Topography filter* values (20 or 10 instead of default 100) and higher *Inverse CMP Offset power* (0.90 instead of default 0.50). DeltatV / XTV starting model for dataset P1-1A is gridded using *Nearest Neighbor method* while the rest of the results are gridded with default Kriging method. As for WET inversion, P1-1A was inverted with Single Run module and 77 iterations but all other results were obtained using Multirun WET and various parameter values. Mostly, the parameters used are similar to the ones we did, but the main differences refer to higher number of *Conjugate Gradient iterations* (15 instead of default 10), 3 *Line Search iterations* instead of default 2, lower *cosine-squared power weighting function* parameter b (7 or 8 instead of default 10), a more steeply descending Wavepath *Width* percentage (30 % to 6 % instead of 30 % to 21 %), a higher *Gaussian width* value (5.5 sigma instead of default 3.0) and higher Damping (0.5 for A, 0.9 for B, C and D).

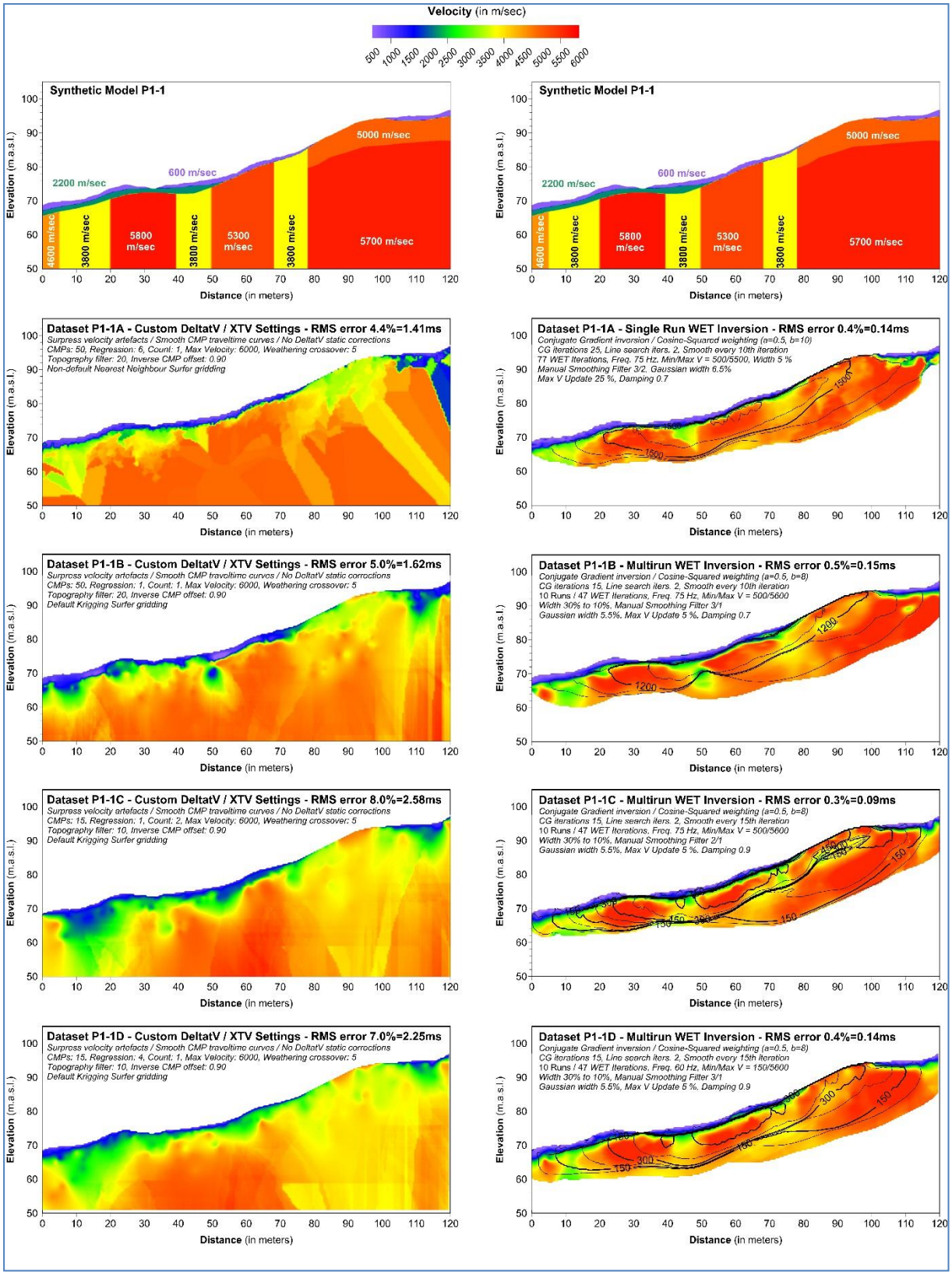

Figure 4.5.1: *DeltatV / XTV results for synthetic data P1-1A, -B, -C and -D obtained from model P1-1 shown on top. To the left: starting models using the same DeltatV parameters. To the right: Single-run (P1-1A) and Multirun (P1-1B, -C and -D) WET inversion results using the DeltatV starting models. Contours represent ray coverage for each WET inversion result.*

Left hand in **figure 4.5.1** shows that DeltatV / XTV application in the creation of a starting model for line P1-1 is not yielding very successful results, regardless of the S. Rohdewald's more knowledgeable approach. All starting models present a low-velocity concentration at the beginning of the profile (lower than modeled), a wide medium-velocity area at the end and several "tongue"-like lows that could be attributed to the central fracture zone but are not continuous with depth. No zones could be interpreted at this stage. Moving on to the inversion results on the other hand, a much better view than at the first attempt is revealed. All three zones are now discernable in all results and a good qualitative interpretation could be done. Nonetheless, none of them is imaged properly in dimensions, verticality and modeled velocity. This shows that with expert-level knowledge of Rayfract®, fracture zones can become at least detectable with the use of DeltatV + XTV starting model. However, inversion results are still not helpful towards interpreting quantitative characteristics for the modeled zones. In addition, the WET inversions seem to underestimate the soil thickness and are not able to indicate the 2200 m/s second soil layer. If we also consider that this is dense synthetic data without any noise added, it appears that conditions such as the ones apparent in model P1-1 present a big challenge also for DeltatV / XTV method.

Figure 4.5.2 follows the same structure as **figure 4.5.1** and presents the results of S. Rohdewald's processing efforts (starting model generation and WET inversion) on all synthetic data produced for model P1-6/7. It is easily concluded here that these results are much better than the ones previously achieved (Figure 4.4.1). The activation of XTV leads to the clear detection of the double zone modeled in both DeltatV / XTV starting model and WET inversion result for all datasets regardless of receiver / shot point density. Concerning DeltatV settings, the parameters in this case are more consistently used i.e. are kept constant with all 4 datasets: *CMP curve stack width* equal to 30, *Regression over offset stations* equal to 6 and *Weathering sub-layer count* equal to 1. However, it is the activation of XTV and the specific *Static first break corrections* variation in S. Rohdewald's processing that achieves the modeled fracture zone's detection. Specifically, the use of *Topography filter* equal to 15 and *Inverse CMP offset power* equal to 0.20 or 0.10 in connection with XTV activation creates starting models where the zone below the low-velocity basin is detectable with the DeltatV.

Nonetheless, a difference in quality is noticeable as the synthetic data becomes more sparsely modeled. The DeltatV / XTV calculated velocity for the fracture zone is closer to the modeled value (2500 m/s) when 1 m of geophone spacing is utilized, whereas when receivers are placed every 2 m, this value drops to 1000 m/s for the whole body of the detected low-velocity vertical concentration making the zone to appear unified with the basin. Moreover, the detected zone acquires the shape of an inverted triangle which means that the zone is thinning in depth. This is not valid in the P1-6/7 model where the zone is vertical throughout the depth. Finally, low-velocity artefacts where high-velocity bedrock is modelled can be observed in all DeltatV / XTV results as expected.

Right side in **figure 4.5.2** shows Single-Run WET inversion results on all synthetic datasets using the DeltatV / XTV output as starting models. WET inversion parameters used are generally not varying too much among the different datasets, and all the outcomes are pretty close to the P1-6/7 model. However, some degrading DeltatV / XTV characteristics are inherited by the inversion results i.e. the inverted triangle shape of the fracture zone and its underestimated velocity when 2 m geophone spacing

is used. Regardless, most artefacts are suppressed in the inversion results and the basin is imaged quite well. Therefore, as opposed to our first results, expert-level knowledge of Rayfract can lead to successful DeltatV / XTV starting models and subsequent WET inversion results as long as we are talking about densely collected refraction seismic data and fracture zones of significant width. DeltatV and XTV settings and parameters are documented in our rayfract.pdf help (Rayfract 2018b).

Another artificial effect seen in the WET inversions in Figure 4.5.2 is a third layer that can be interpreted as weathered bedrock which shows a velocity of ca. 3000 m/s (green velocity values). This seems to be a combined result of the second soil layer (1800 m/s) and the weathered bedrock (4900 – 5000 m/s). The effect of this is underestimation of the soil thickness since 3000 m/s do not represent soil material.

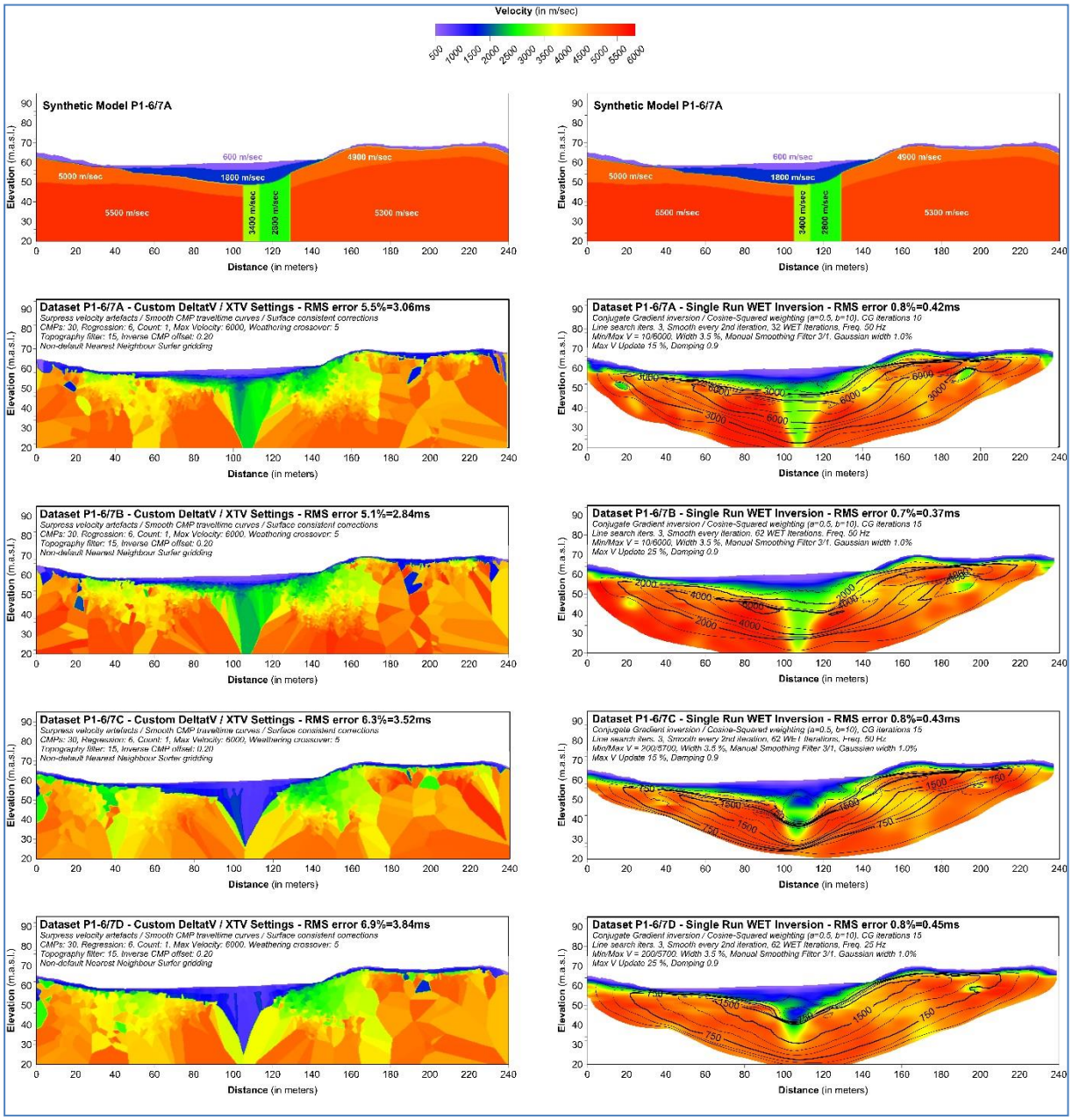

Figure 4.5.2: *DeltatV / XTV results for synthetic data P1-6/7A, -B, -C and -D obtained from model P1-6/7 shown on top. To the left: starting models using the same DeltatV parameters. To the right: Multirun WET inversion results using the DeltatV starting models. Contours represent ray coverage for each WET inversion result.*

5. HAGEDOORN'S PLUS-MINUS METHOD APPLICATION

As shown in Tassis et al. (2017), the application of Hagedoorn's Plus-Minus method with the use of interactive picking of branch points in Rayfract® can work in detecting fracture zones in bedrock. Considering that the same models P1-1 and P1-6/7 were employed in that study but with much sparser receiver/shot spacing (5 m / 30 m respectively), we expect that the much denser arrays utilized for this report will yield even better results. In this context we present here the procedure of creating starting models for all our synthetic data with the use of Plus-Minus method and the results obtained after running multirun WET inversion.

5.1 Plus-Minus starting models for P1-1

Rayfract® allows to create sophisticated starting models. You manually assign traces to refractors by interactively picking branch points for single shot-sorted traveltime curves as shown in **figure 5.1.1**. These branch points are used to separate refractors. The maximum number of refractors that can be assigned to a single shot is two which means three layers in total. However, this can pose a problem for cases such as the one in model P1-1. The model contains various vertical variations in velocity and only two of those can be mapped in this way. However, prior knowledge of the model helped us to pick the branch points considering the actual change in velocity these layers represent. Models with denser receiver/shot spacing offer a larger number and more detailed traveltime curves enabling easier branch point picking. **Figure 5.1.1** shows dataset P1-1A which is the densest for model P1-1 and how picking of branch points looks like inside Rayfract®. White rectangles represent the branch point between the direct wave of 600 m/s (shown in yellow) and the refracted wave from the underlying ca. 2200 m/s overburden (shown in red). Black rectangles mark the branch points between the 2200 m/s overburden from the ca. 5000 m/s bedrock (shown in green) underlying it. Green colors represent a single body with velocity of ca. 5000 m/s (bedrock) lying beneath the other two soil layers. The bedrock can be laterally differentiated by changing the *Smoothing overburden* and *base filter parameters* of the Plus-Minus method (Rayfract 2018b). Default value for these filters is 10 and 15 but decreasing them can fragment the "green" layer in **figure 5.1.1** in a way that it resembles vertical fracture zones.

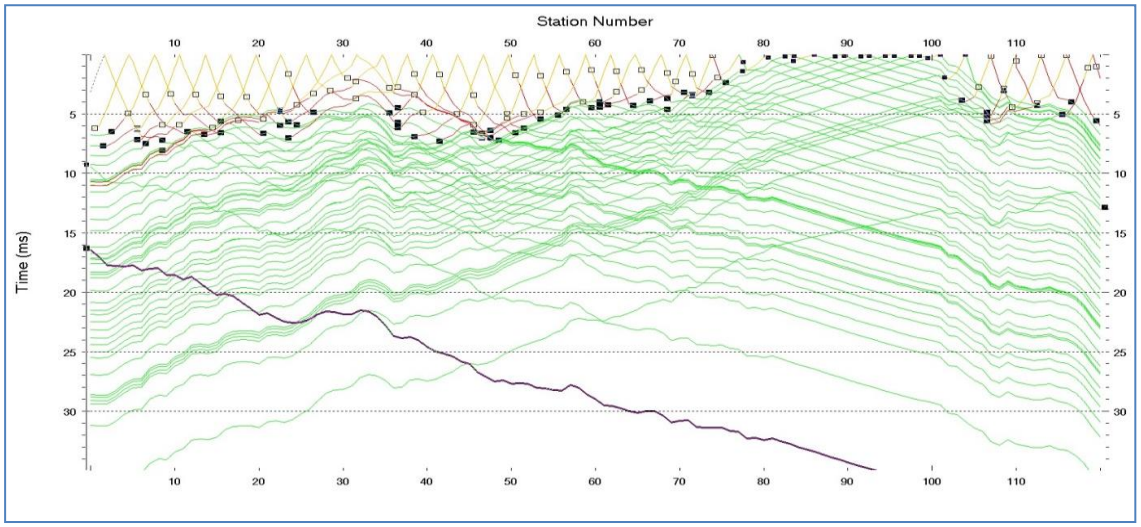

Figure 5.1.1: *Interactive picking of branch points for dataset P1-1A.*

The interactive picking of branch points was repeated for all P1-1 datasets (A to D) and *Smoothing overburden* and *base filter* values were adjusted to achieve the best result. **Figure 5.1.2** shows the Plus-Minus method results together with the actual model (top left) and the result obtained in 2017 with receiver/shot spacing equal to 5 and 30 m respectively (top right). It must be noted that the 2017 result was obtained with only one branch point picked since the low geophone and shot coverage did not allow a second one to be picked. The branch point picking was not perfect due to the lack of time and the big number of individual traveltime curves therefore, some slight mismatches from the P1-1 model are noticeable.

Assigning traces to refractors is neither an easy nor a quick task, but the merit in doing so is great and that is proven by the results shown in **figure 5.1.2**. Regardless of the fact that our synthetic model is favorable for imaging using Plus-Minus method (discrete blocks, perfectly vertical fracture zones, uniform velocities), the results obtained are extremely accurate both in qualitative and quantitative terms. All zones are standing out clearly and even the challenging limit at around 5 m source - receiver distance is distinguishable. The overburden layers are also mapped with high accuracy and their limits are as sharp as they were modeled with small deviations which are due to imperfect branch point picking.

The vertical velocity variation in bedrock at the last part of the profile (5000 m/s on top of 5700 m/s) is difficult to visualize using Plus-Minus method in Rayfract®. Furthermore, a full multirun WET inversion with nine iterations for dataset P1-1A takes about 50 minutes to complete using a 64 bit Laptop with 2.7 GHz processor and 16 GByte RAM. Therefore, an effort to map this refractor was made only on dataset P1-1D which has the fewest shot points and therefore WET inversion is faster to run. We attempted to use the second available branch point to map the clear refractor seen along the last traveltime curves of the profile and mark the limit between the 600 m/s overburden and the bedrock formation below (5000 m/s). At the beginning of the profile the second branch point was used to mark the 2200 m/s layer which is not continued past the centre of the profile. This has resulted in a layer which is not very accurate in relation to the model (different shape, smaller thickness, lower velocity) but showcases the possibilities given by Hagedoorn's Plus-Minus method in Rayfract®.

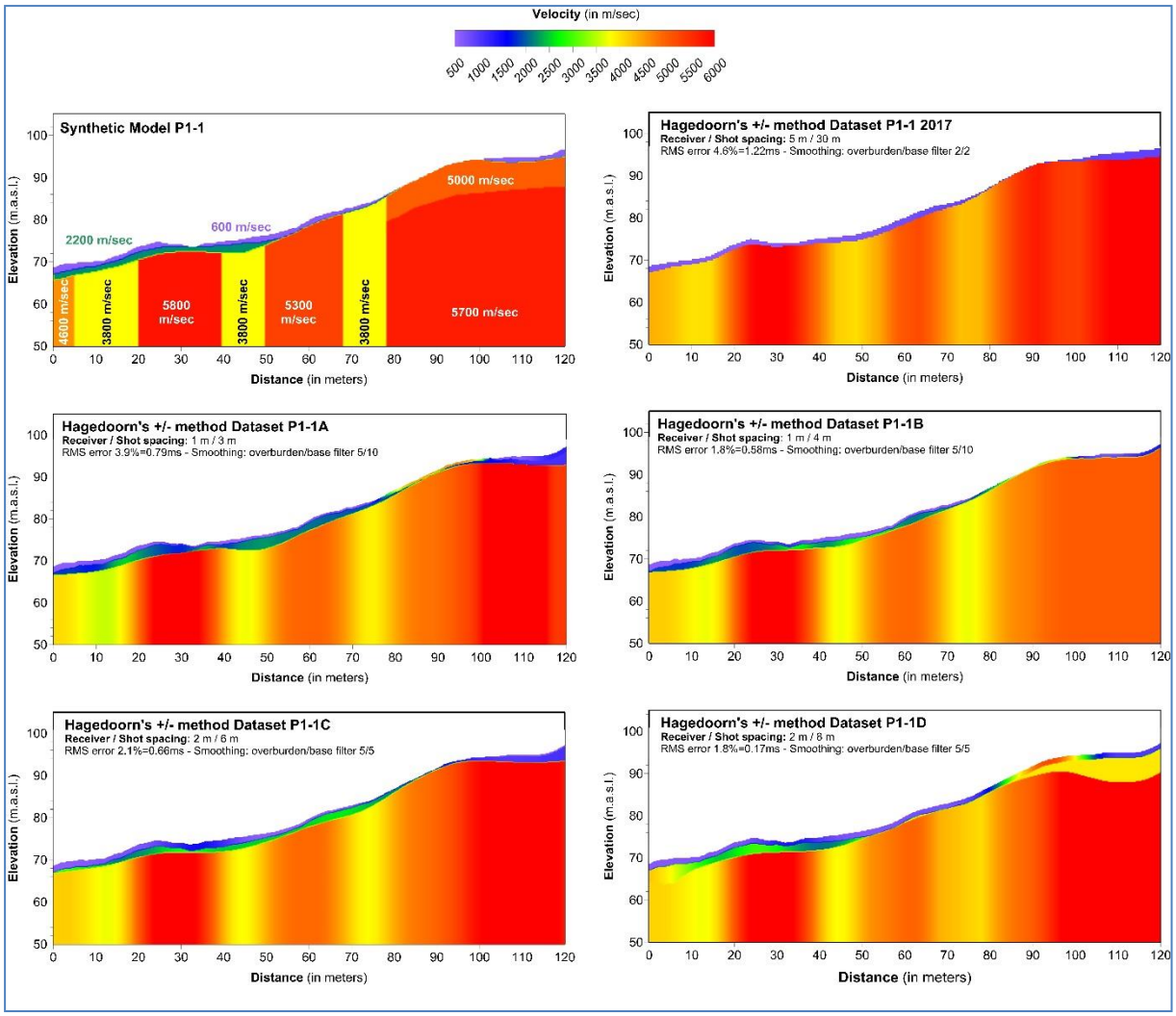

Figure 5.1.2: *Hagedoorn's Plus-Minus method obtained starting models for model P1-1 (top left). Presented in this figure are: P1-1 dataset from 2017 (geophone spacing 5 m, shot spacing 30 m, top right), dataset P1-1A (mid left), P1-1B (mid right), P1-1C (bottom left) and P1-1D (bottom right).*

5.2 WET inversion with P1-1 Plus-Minus starting models

As already mentioned, the accuracy of the starting models is almost quintessential for the success of WET inversion. At the same time, Rønning et al. (2016) and Tassis et al. (2017) have shown that given the nature of the models (compact blocks, uniform velocities, vertical limits), Plus-Minus method may return a better result than WET inversion. However, our models do not represent reality but rather an oversimplification of it for investigation purposes. In any case, **figure 5.2.1** shows that when receiver/shot point spacing is dense, WET inversion can image such models very accurately.

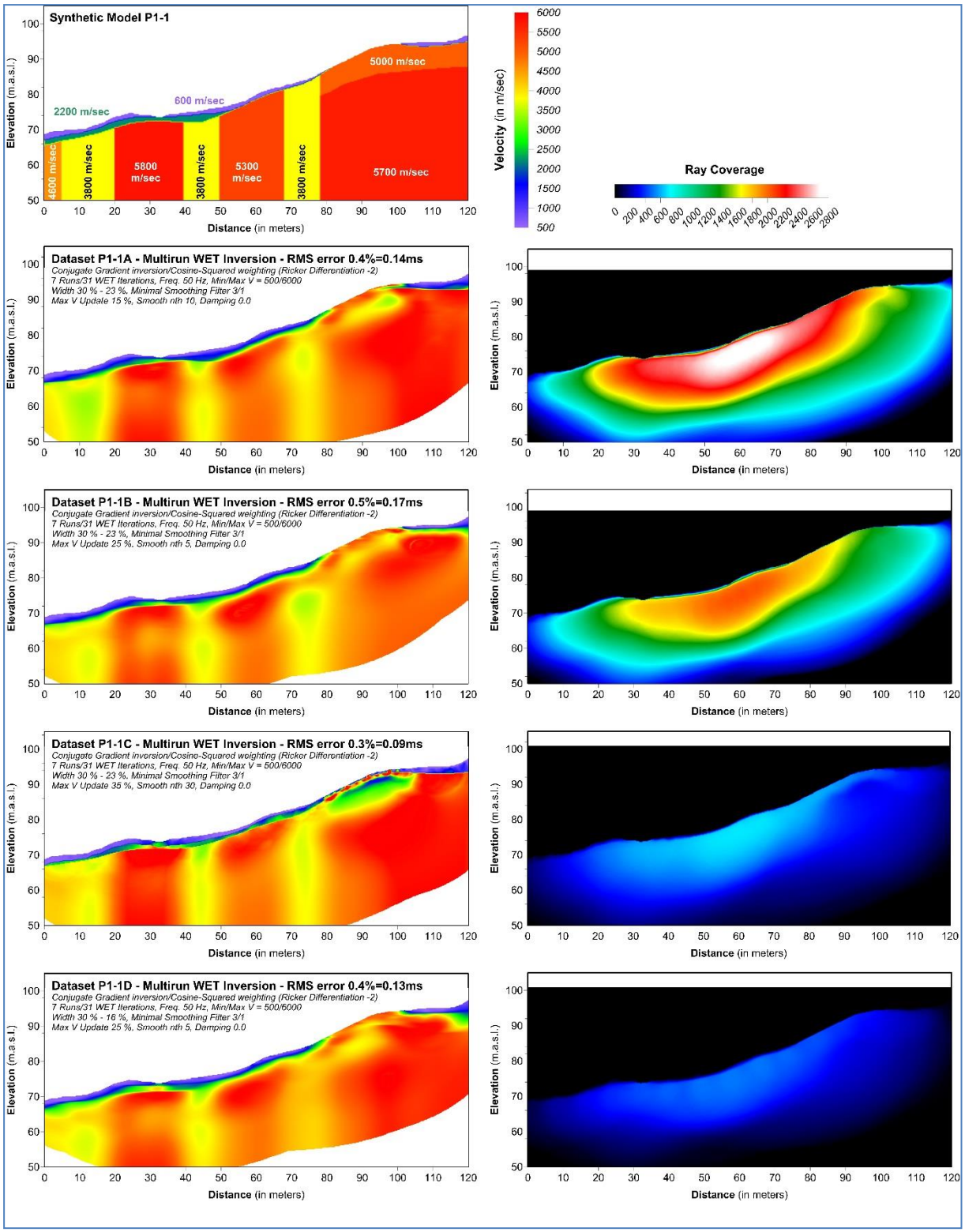

Figure 5.2.1: *Left: WET inversion results for datasets P1-1A, -B, -C and -D using Plus-Minus starting models derived for each and Conjugate Gradient WET inversion /Cosine -Squared weighting. Right: Ray coverage for each inversion result.*

All profiles were inverted using *Conjugate Gradient* inversion, *Cosine-Squared* weighting, 7 *WET runs*, 50 Hz *Frequency*, *Multirun WET with Wavepath width* decreasing from 30 % to 16 % and *variously minimized smoothing*. The extent of smoothing minimization is generally limited but also slightly increased for the less dense geophone/shot datasets. The results shown in **figure 5.2.1** have been produced

with only a few attempts but their quality is high. Essentially, this means that using dense arrays in collecting refraction seismic data provides better conditions for accurate WET inversion without having to resort to extremely minimized smoothing as in Tassis et al. (2017). As seen on the left-hand side of **figure 5.2.1**, the modeled fracture zones are accurately detected. Inversion may have caused some of them to lose their sharp vertical borders and show gradual decrease in velocity towards their center, but this is something more probable to happen in nature rather than coming across completely uniform and perfectly-shaped weak zones. Wherever denser shot points are available (P1-1A and -B), bedrock velocity is more accurately calculated whereas the vertical velocity variation within bedrock at the end of the profile is imaged - although inaccurately - where ray coverage is greater (right-hand side **figure 5.2.1**). Lastly, all overburden layers are detected in detail although the bottom overburden layer (2200 m/s) at the beginning of the profile is sometimes unified where it meets fracture zones.

5.3 Plus-Minus starting models for P1- 6/7

Synthetic dataset P1-6/7A incorporated 84 shot points and **figure 5.3.1** shows how picked branch points along twice as many traveltime curves (forward and backward) look like in Rayfract®. Prior knowledge of model P1-6/7 has safely steered refractor mapping in accordance to it and therefore, yellow colors represent the direct rays of the overburden layer (600 m/s), red refers to the bottom overburden of the basin in the middle (1800 m/s) and green to the underlying bedrock (5000 m/s top, 5500 m/s bottom). High receiver/shot spacing for this synthetic dataset enables the Plus-Minus method to separate the two sub-layers that the sedimentary basin consists of, as opposed to the 2017 result where a uniform velocity equal to 700 m/s and an underestimated thickness was calculated for the entire basin. It is also interesting to discern whether higher geophone/shot point coverage can help with detection of both adjacent zones below the basin in model P1-6/7 or if the result still is a unified area with a mean velocity between the two modeled values.

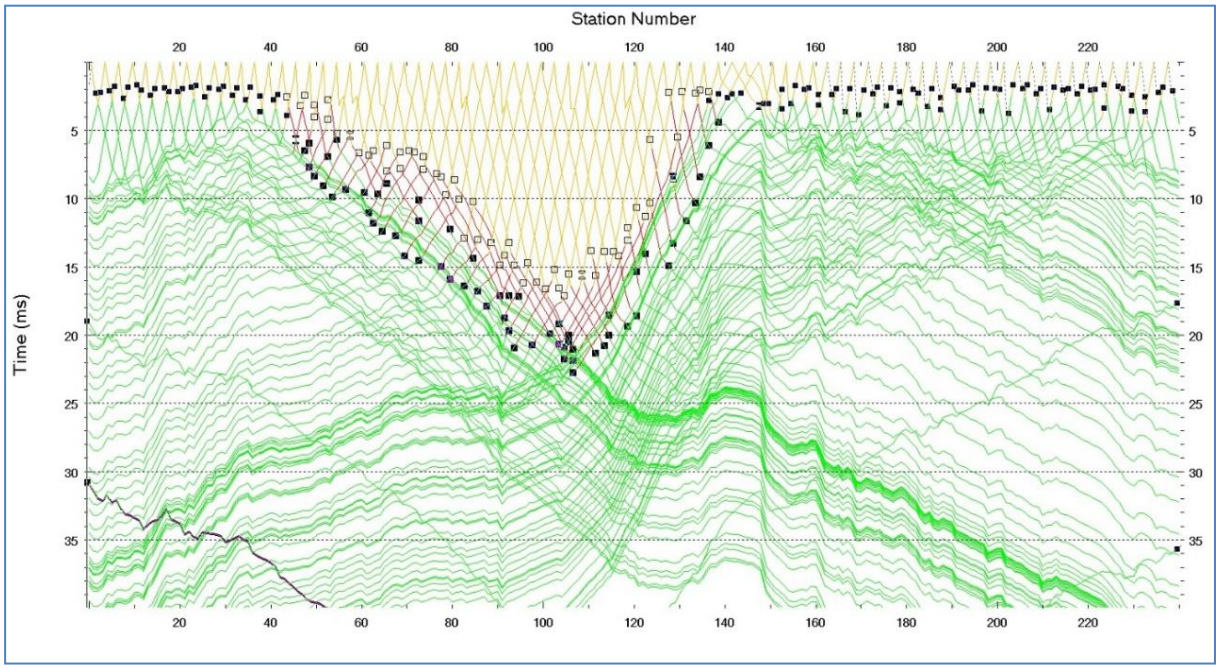

Figure 5.3.1: *Interactive picking of branch points for dataset P1-6/7A (receiver spacing 1 m, shot spacing 3 m).*

Figure 5.3.2 shows the starting models obtained with Hagedoorn's Plus-Minus method for datasets P1-6/7A (middle left), P1-6/7B (middle right), P1-6/7C (bottom left) and P1-6/7D (bottom right). The figure also contains the synthetic model (top left) and the 2017 result for a dataset with sparser receiver/shot spacing (5 m/30 m, top right). All new datasets were processed with the same *Smoothing overburden filter* and *base filter* value i.e. default 10 for both parameters. The intent behind this was to highlight the effectiveness of this parameter in laterally separating bedrock and thus revealing possible fracture zones. As shown in the middle part of **figure 5.3.2**, datasets P1-6/7A and -B with high geophone coverage (1 m) can enable Plus-Minus to separate the two modeled adjacent zones even with default settings, although not accurately. However, this is accompanied by further high fragmentation and possible fracture zones appearing in places where uniform velocities should be mapped like between 10 and 20 m distance on both profiles and the middle of the basin for dataset P1-6/7B. We will see if such light fragmentation affects WET inversion in the next section.

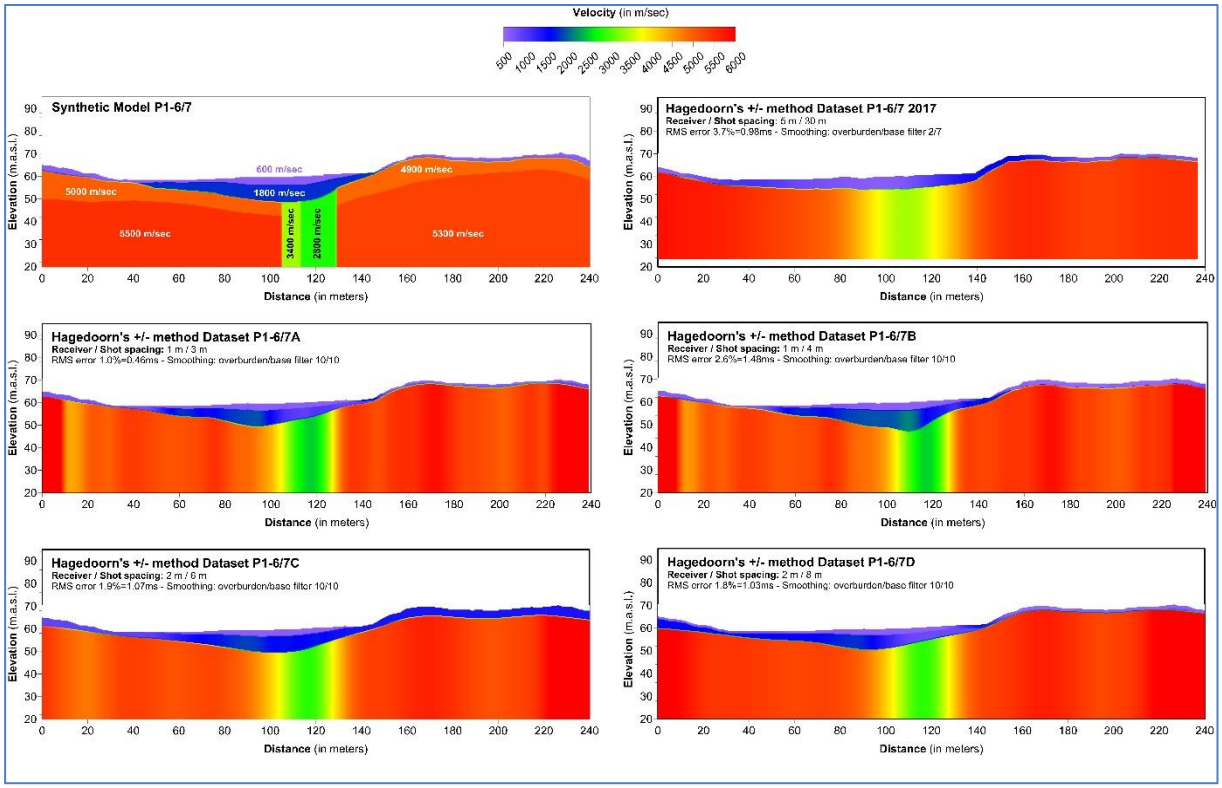

Figure 5.3.2: *Hagedoorn's Plus-Minus method obtained starting models for model P1-6/7 (top left). Presented in this figure are: P1-6/7 dataset from 2017 (top right), dataset P1-6/7A (mid left), P1-6/7B (mid right), P1-6/7C (bottom left) and P1-6/7D (bottom right).*

The bottom part of **figure 5.3.2** shows how the same filtering values affect Plus-Minus when geophone spacing is 2 m like in datasets P1-6/7C and -D. Default settings combined with lower receiver coverage in these two datasets, yield one single zone instead of two with a velocity rapidly dropping from 3700 m/s at the edges until it settles over the largest portion of the zone at 2900 m/s. This calculation is equivalent to the 3400 and 2800 m/s two-zone setting in model P1-6/7 but doesn't have the resolution to separate these two zones. Similar results are obtained for datasets P1 -6-7A and -B when setting *Smoothing overburden* and *base filters* to 20. Although the resolution

these dense datasets offer can be mimicked for datasets P1-6/7C and -D by lowering the filtering parameters even to 2 which is the lowest allowed by Rayfract®, bedrock becomes too fragmented with many artefact zones emerging that could ruin WET inversion.

In any case, Plus-Minus method results are very close to the synthetic model P1-6/7 as shown by the extremely low RMS errors obtained (2.6 % and less). If we compare the new datasets with the 2017 one which was compiled using 5 m receiver and 30 m shot spacing (top right in **figure 5.3.2**), we can observe that the detected low-velocity area below the basin is more compact in all new results and that the overburden imaging is far more accurate. The two sub-layers which build up the basin are sharply separated while their calculated velocities are equal to the modeled ones. The 2017 dataset does not allow the detection of two adjacent zones like in the synthetic model even with *Smoothing overburden* and *base filter* set to 2 and 7 respectively. Also, Plus-Minus method cannot image the vertical velocity variation in bedrock neither for the 2017 nor the newer datasets. This is an issue for WET inversion to resolve.

5.4 WET inversion with P1-6/7 Plus-Minus starting models

Figure 5.4.1 shows multirun WET inversion for datasets P1-6/7A, -B, -C and -D, using as starting models the Plus-Minus respective profiles shown in **figure 5.3.1**. Results are shown with their respective ray coverage graphs to highlight which part of the inversion is more reliable i.e. is based on more ray paths. Multirun WET inversion with 9 iterations takes about 55 minutes for dataset P1-6/7A which is the densest. We employed the same WET inversion parameter combination for all four synthetic datasets i.e*. Multirun Conjugate Gradient* inversion, *Cosine-Squared* weighting, 31 WET iterations per run, 7 *WET runs* 50 Hz *Frequency*, *Multirun* WET with *Wavepath width* decreasing from 30 % to 16 % and minimized smoothing with *Maximum Velocity update* equal to 35 % and *Smooth iteration number* equal to 20.

As seen in **figure 5.4.1**, WET inversion results do not differ much from the Plus-Minus starting models. Results for datasets P1-6/7A and -B with starting models containing a hint of a double zone below the basin, continue to detect this pattern but not continuously in depth. The largest area of the detected low-velocity concentration presents a value around 3000 m/s which is equivalent to the two modeled zones (first zone 10 m wide / 3400 m/s, second zone 15 m wide / 2800 m/s) while the accumulated fracture zone width (25 m) is calculated accurately and sharply in all results. Also, the basin's qualitative and quantitative characteristics are defined very well with small variations between each synthetic database, depending on how accurately branch point were picked at the Plus-Minus method application stage. Small discrepancies arise from inaccurate picking due to lack of time as for model P1-1.

Regarding vertical variation in bedrock velocity apparent throughout model P1-6/7, we can say that WET inversion returned results whose success is depending on the amount of fragmentation caused by the choice of filtering for Plus-Minus method interpretation. Datasets P1-6/7A and -B follow up with this relatively high lateral variation seen in their starting model but a lower bedrock velocity is indeed calculated for shallower depths. Such a variation in bedrock is also detected in datasets P1-6/7C and -D if only locally exaggerated, especially with the latter (various small areas of velocity underestimation). The choice of a starting model such as obtained with

Hagedoorn's Plus-Minus method can steer WET inversion in good and bad directions alike, depending on its accuracy or caused artefacts. Denser recording arrays yield results with higher ray coverage which means higher reliability.

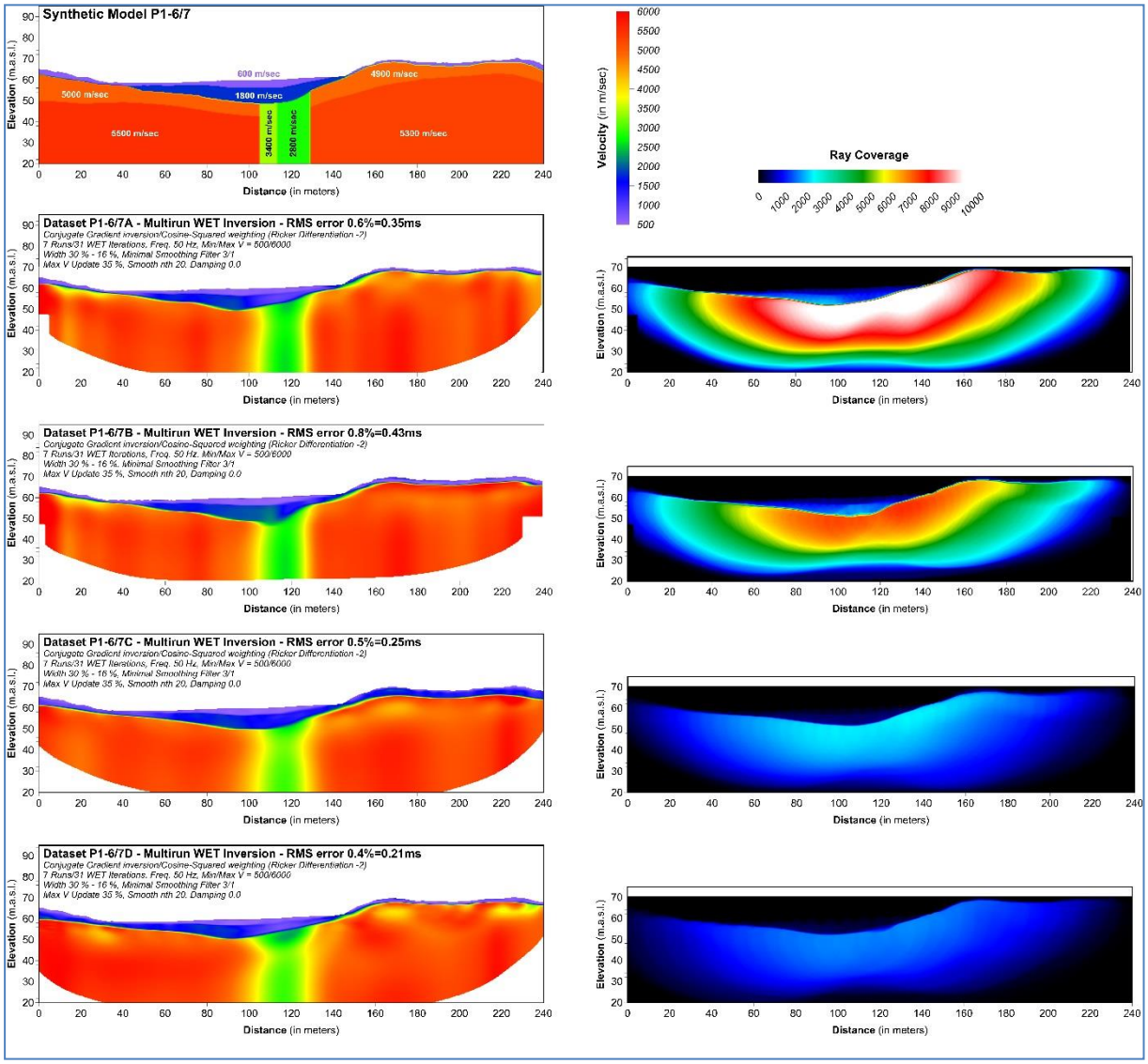

Figure 5.4.1: *Left: WET inversion results for datasets P1-6/7A, B, C and D using Plus-Minus starting models derived for each. Right: Ray coverage graphs for each inversion result.*

6. ALTERNATIVE WAVEFRONT & PLUS-MINUS METHOD APPLICATION

In this section we present another method to create starting model using picked branch point, the Wavefront method. We present also another way of producing a starting model without the use of interactive branch point picking but with the use of midpoint breaks i.e. CMP-sorted traveltime curves (Rayfract 2018b, chapter Mapping traces to refractors). This procedure was proposed by Rayfract® developer S. Rohdewald and is presented here to show how to create a starting model without having to go through the time- consuming procedure of manually picking branch points. This procedure will only be applied on the most detailed synthetic dataset available for each.

The Wavefront method can be considered as an optimized version of the GRM (Generalized Reciprocal Method) algorithm described by Palmer (1980). Instead of assuming a user-specified constant receiver separation ("XY distance", "Optimum XY value") all along the profile, the Wavefront method automatically estimates the local receiver separation at each receiver station from local forward and reverse wavefront emergence angles. Plus-Minus which was tested in the previous sections has a theoretically lower lateral resolution when compared to the Wavefront method, because it basically assumes that critically refracted rays emerge vertically from the refractor. The error caused by this assumption increases with increasing overburden thickness or decreasing velocity contrast, between the layer above the refractor being mapped and the refractor itself (Rayfract 2018b). Since we are investigating vertical structures we want to investigate if Wavefront method can provide better starting models than Plus-Minus method.

6.1 Wavefront application using branch points

Interactive picking of branch points enables using both Plus-Minus and Wavefront methods. So far, we have only presented the Plus-Minus results but since all branch points are already picked and Wavefront method was not investigated in previous NGU reports, it was interesting to test the method under the best given conditions i.e. on datasets with very dense receiver/shot point spacing. Applying Wavefront is just a matter of choosing the *Depth/Wavefront* menu option instead of the *Depth/Plus-Minus* one in Rayfract® once traces has been mapped to refractors. The calculation of the result requires the same *Smoothing overburden* and *base filter* parameters as in Plus-Minus for the lateral variation degree to be decided.

Figure 6.1.1 shows Wavefront method results for datasets P1-1A and P1-6/7A (middle) using the same branch points along with the Plus-Minus result (bottom) and the synthetic models (top). To obtain similarly successful results as with Plus-Minus method for dataset P1-1A, *Smoothing overburden* and *base filter* values for Wavefront had to be modified to 10 and 5 respectively. Using these parameters, Wavefront returns results which are quite similar to Hagedoorn's Plus-Minus result and pretty accurate compared to the synthetic model. However, in strict qualitative and quantitative terms, the Plus-Minus model is superior to the Wavefront result even though the branch points were exactly the same. All three fracture zones are detected with both methods but the Plus-Minus zones are better imaged, and their velocity is more accurately calculated. Wavefront seems to underestimate the velocity of the first zone and neighboring space, detects the middle zone but with less intensity and finally presents several artificial effects around the third weak zone.

Right-hand side of **figure 6.1.1** shows that the same observations can be made for dataset P1-6/7A results too. It is noted that this time, Wavefront yielded its best results with *Smoothing overburden* and *base filter* values equal to 5 and 10 respectively. Nonetheless, the result obtained is again not preferable over the Plus-Minus outcome especially when zone detection accuracy is sought. Using the Wavefront method, the modeled pair of zones in model P1-6/7 is detected as one zone but with smaller width i.e. 15 m instead of 25 m. Furthermore, the area surrounding the zone is also underestimated in velocity while the zone's value is returned somewhat higher (3100 m/s) to compensate for the zone thinning. Overburden calculation seems to be unaffected by the use of either Plus-Minus or Wavefront method for both models.

Therefore, when branch point picking is taking place, Hagedoorn's Plus-Minus method is still the preferable choice. Despite of being a method for creating a starting model, the Plus-Minus model may be used as the final inversion result.

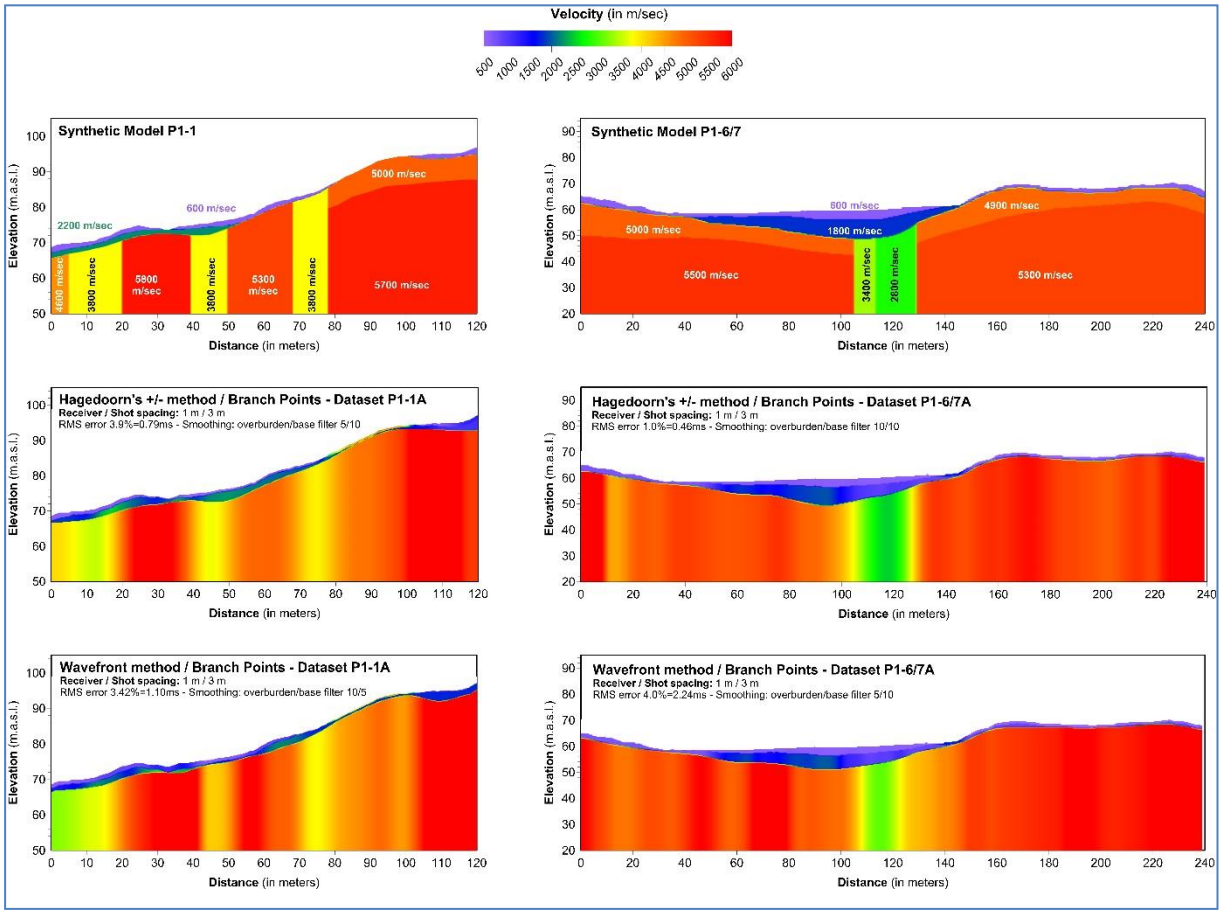

Figure 6.1.1: *Starting models for dataset P1-1A (left) and P1-6/7A (right) with the use of interactive branch point picking and depth conversion using Plus-Minus (middle) and Wavefront (bottom) methods.*

Figure 6.1.2 shows the multirun WET inversion result after using the starting models shown in **figure 6.1.1**. The WET inversion parameters selected are listed with each profile in the figure and are kept constant for each synthetic model. The differences between the obtained results are almost imperceptible and those parts that are indeed different are due to discrepancies in the starting models which are inherited in the inversion results. For dataset P1-1A, using Wavefront method to generate a starting model does not enable WET inversion to distinguish the lateral velocity variation at the beginning of the profile, while the bedrock block following next is shown horizontally fragmented by low-velocity artefacts. The results for the simpler synthetic model P1-6/7A on the other hand are almost identical. This essentially means that successful picking of branch points leads to small differences between the application of Plus-Minus and Wavefront method. Still, Plus-Minus method returns slightly better results for more complex subsurface conditions.

At line P1-6/7, the two soil layers with velocities 600 m/s and 1800 m/s show up almost exactly as they are in the synthetic model. At line P1-1 it seems difficult to pick up the 2200 m/s soil layer. It is partly seen in both starting models (Figure 6.1.1) but disappears in the WET inversion. The total soil thickness seems to be acceptable.

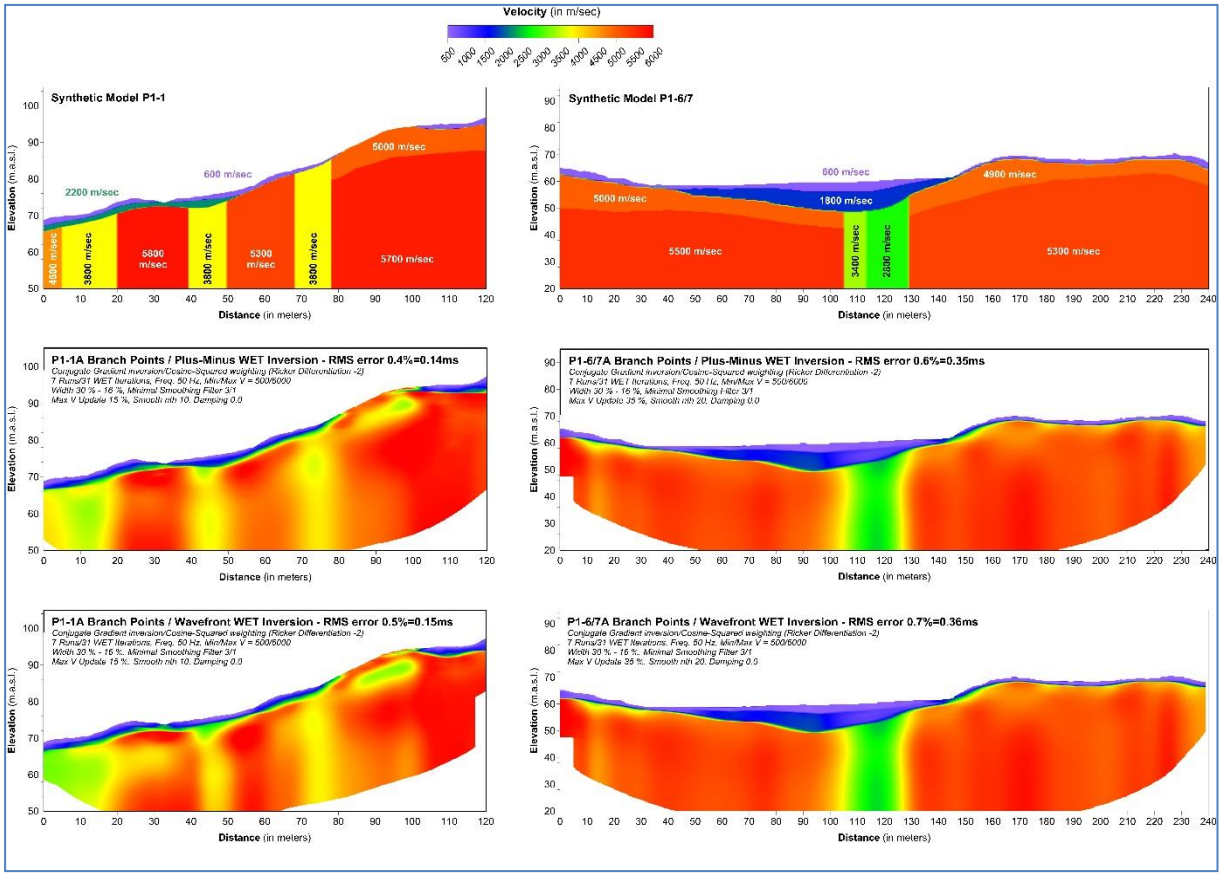

Figure 6.1.2: *Multirun WET Inversion results with starting models obtained from branch point picking using Plus-Minus (middle) and Wavefront (bottom) method for synthetic datasets P1-1A (left) and P1-6/7A (right). The synthetic models are shown at the top.*

6.2 Wavefront and Plus-Minus application using midpoint breaks

In the communication with Rayfract® developer S. Rohdewald, he has informed us that Wavefront and/or Plus-Minus methods do not necessarily need branch point picking to be applied in the program. Instead, he has given us guidelines and a set of suggested parameters to apply these methods by using mapping of midpoint breaks (Rayfract 2018b, chapter Mapping traces to refractors). To do so, our data had to be exported and re-imported for correcting shot stations for shot inline offset. This correction is done automatically by Rayfract® when exporting first breaks, station and shot point coordinates.

The suggested midpoint break processing contained the following steps: unchecking of *Direct wave first breaks recorded* option, setting *Refractor Count* to 2 *CMP Stack Width* to 28, *Refracted Wave Offset Delta* to 3, *Weathering limit* to 1000 m/s, *Refractor 1 limit* to 1800 m/s and subsequent mapping of traces. Before running Wavefront and Plus-Minus methods, soil cover velocity had to be reset for all stations to 600 m/s and 1800 m/s accordingly to each model. *Smoothing overburden* and *base filter* values were kept the same as in **figure 6.1.1** for each respective dataset.

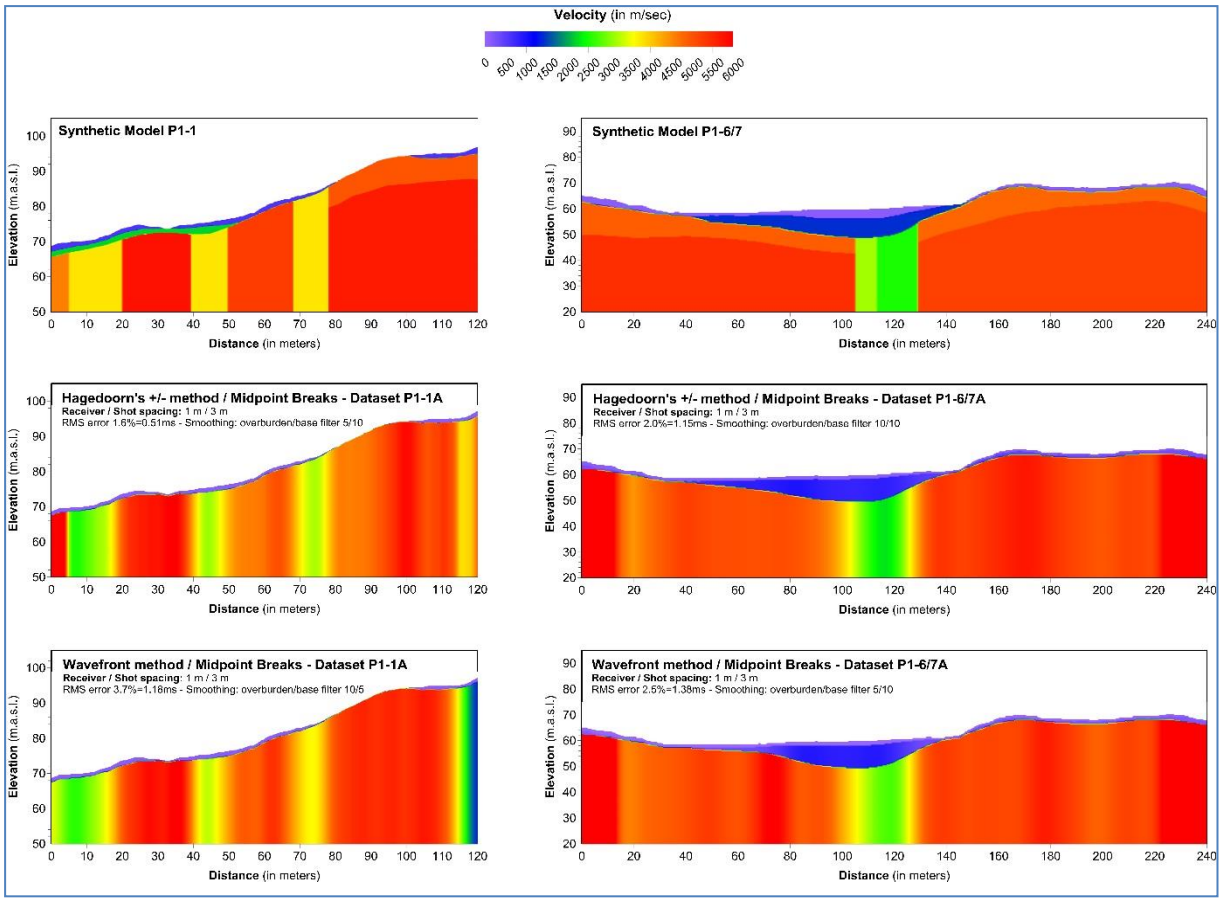

Figure 6.2.1: *Starting models for dataset P1-1A (left) and P1-6/7A (right) with the use of midpoint breaks mapping and depth conversion using Plus-Minus (middle) and Wavefront (bottom) methods. The synthetic models are shown at the top.*

Semi-automatic Plus-Minus and Wavefront method application with the use of midpoint breaks returns results which are quite similar to the ones obtained with branch point picking. **Figure 6.2.1** displays some minor differences which indicate that mapping midpoint breaks can give fast and relatively accurate results but picking branch points is giving slightly more sensible results because of its interactive character. For dataset P1-1A, both Plus-Minus and Wavefront detect all fracture zones but with underestimated velocities while the overburden is not as detailed. For dataset P1-6/7A, zone detection is as successful as with branch point picking but the top-layer's thickness with velocity 600 m/s is underestimated. At dataset P1-1 the total thickness of the overburden is underestimated and the 2200 m/s layer is absent. Furthermore, all datasets (P1-1A especially) yield results with artefacts near their edges which do not affect WET inversion since ray coverage resulting from the recording geometry is not adequate in those areas and therefore features at the edges of profiles are discarded. Using overlapping receiver spreads (Rayfract 2018b) to extend the profile is recommended.

Figure 6.2.2 shows multirun WET inversion results using midpoint breaks generated starting models shown in **figure 6.2.1**. The results here are almost identical to those obtained with branch point picking but also slightly inferior. This is because midpoint breaks option is an almost automatic procedure which in our case has underestimated zone velocities, was unable to accurately distinguish the correct thickness for each

horizontal layer in the overburden for dataset P1-6/7A, did not pick up the 2200 m/s soil layer in dataset P1-1 and presented artefacts at the edges of the profile especially for dataset P1-1A. As expected, these features are all inherited in the WET inversion results, rendering them slightly inferior to their respective branch point picking ones. The interactive character of branch point picking enables the user to be more flexible when creating a starting model and has a higher level of detail when receiver/shot spacing is dense enough.

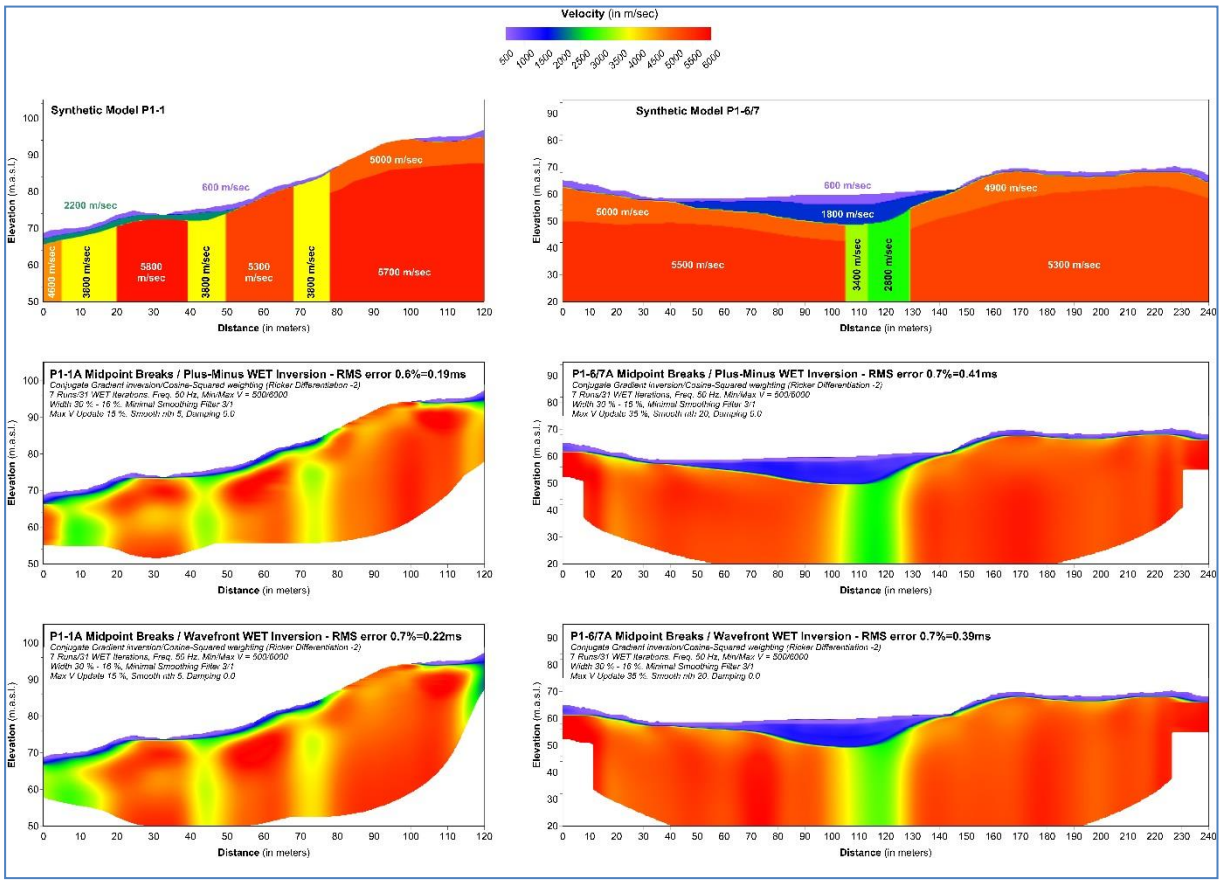

Figure 6.2.2: *Multirun WET Inversion results with starting models obtained from midpoint breaks option using Plus-Minus (middle) and Wavefront (bottom) method for synthetic datasets P1-1A (left) and P1-6/7A (right). The synthetic models are shown at the top.*

7. OVERBURDEN EFFECT IN WET INVERSION

In this section, we will test WET inversion on synthetic data originating from previously presented models with the addition of low-velocity overburdens amounting to either 20 or 40 m. The overburden shape is following topography and consists of a 5 m top layer with velocity equal to 600 m/s and a bottom counterpart, either 15 or 35 m thick with 1800 m/s velocity (see **figure 7.1.1**). All other features included in models P1-1 and P1-6/7 such as fracture zones or internal bedrock structure remain the same. Synthetic data were produced using the same receiver/shot point spacing as in datasets described by letter D i.e. geophones every 2 m, shots every 8 m and two distant shots on every side of each model at a distance equal to a quarter and half the profile's length

(30/60 m for P1-1, 60/120 m for P1-6/7). This was done to simulate almost real conditions in refraction seismic surveying which utilizes less dense arrays than presented in this report due to financial reasons (usually 5 m geophone and 30 m shot spacing). Finally, starting models were created with interactive branch point picking and subsequent Hagedoorn's Plus-Minus method while WET inversion employed parameters simular to those used in previous sections.

7.1 WET inversion on Model P1-1D with overburden

Figure 7.1.1 presents from top to bottom: the P1-1 synthetic model with the overburden layer, the Plus-Minus starting model constructed, the multirun WET inversion result and the ray coverage graph for overburden thicknesses equal to 20 (left) and 40 m (right). Before we take a closer look at the two cases separately, we can again verify how important the starting model is to the ensuing inversion procedure and how ray coverage distribution changes with the increase in overburden thickness.

Left-hand side in **figure 7.1.1** shows results for overburden thickness equal to 20 m. Assigning branch points to traveltime curves and using Hagedoorn's Plus-Minus method, we obtained the starting model shown second from top. Branch point picking led to detailed imaging of the overburden horizons with accurate velocities whereas the underlying fracture zones are detectable although appearing somewhat misplaced with the exception of zone number three. The third profile from the top shown in this figure is the Multirun WET inversion result which is heavily depending on the Plus-Minus starting model and verifies the features detected there. Ray coverage (bottom left figure) displays an investigation depth equal to 40 m with a dense ray concentration (over 1500 rays) around the middle part of the profile and exactly below the overburden. The highest ray coverage (red colors) is matching part of the second and the entire third fracture zone locations and therefore this is the reason why the latter is better imaged than the former (misplaced with a larger inaccuracy extent). The first modeled zone at the edge of the profile lies in a low ray coverage area and therefore cannot be adequately imaged.

Right-hand side in **figure 7.1.1** presents the exact same profile sequence but this time for a 40 m thick overburden. Doubling the overburden thickness has a serious deteriorating effect on all results and a different ray coverage distribution. The Plus-Minus starting model is again imaging the overburden layers accurately but underestimates the bedrock velocity and misplaces/miscalculates zones number one and two while completely failing to detect zone number three. All these effects are propagated to the WET inversion result which is not able to improve the result. Ray coverage may be reaching a higher total depth (50 m) but at the same time presents a non-favorable pattern in the detection of the buried fracture zones. The highest ray coverage is concentrated on the top part of the model where overburden layers are found only while the number of rays travelling through the zones, is low (between 50 and 100). This means that a 40 m overburden is not allowing enough depth resolution for the zones to be detected with WET inversion, even after modeling two far-offset shots per side of each profile with offset of a quarter and half the profile's total length as proposed by S. Rohdewald. More densely spaced long-offset shots or using overlapping receiver spreads (Rayfract 2018b) should probably give a better result.

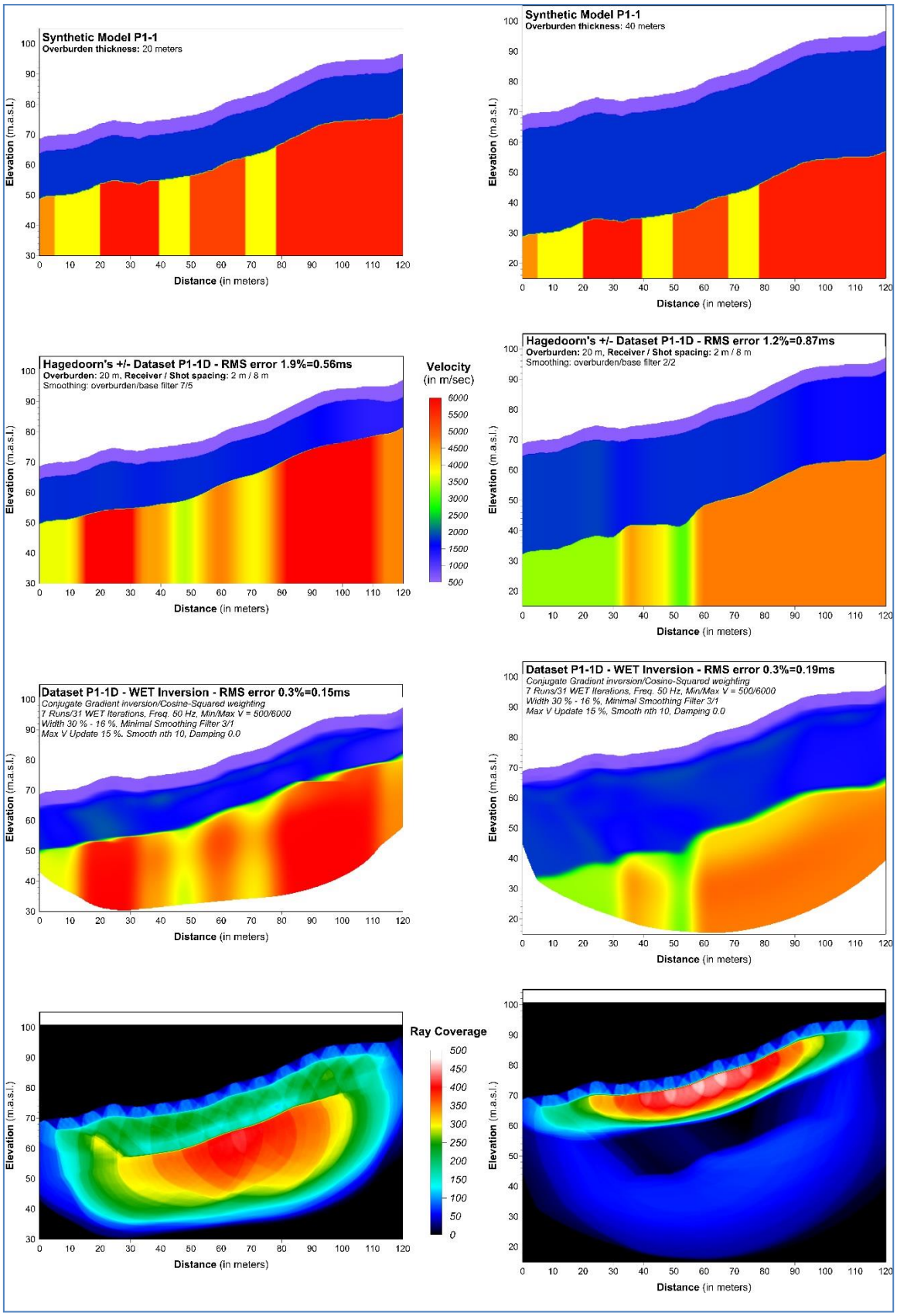

Figure 7.1.1: *P1-1 synthetic model (top), Plus-Minus starting model (second), WET Inversion result (third) and ray coverage graph (bottom) for overburden thickness equal to 20 m (left) and 40 m (right).*

7.2 WET inversion on Model P1-6/7D with overburden

The presentation structure followed in **figure 7.1.1** is also used in **figure 7.2.1**. This time, the 20 and 40 m thick overburdens are added to model P1-6/7 which has twice the length of model P1-1 and therefore offers a larger depth coverage. Left-hand side **figure 7.2.1** (overburden thickness 20 m) displays a good zone detection for both Plus-Minus starting model and WET inversion result, with the latter being able to push its lateral dimensions a bit closer to the modeled ones. Overburden calculation is again very good. Ray coverage shows a maximum imaged depth of 60 m following the same distribution as in the previous case i.e. largest ray concentration (over 1500 rays) found in the middle of the profile and below the soil overburden. This is also the area where the double zone is modeled and therefore, its detection is enabled.

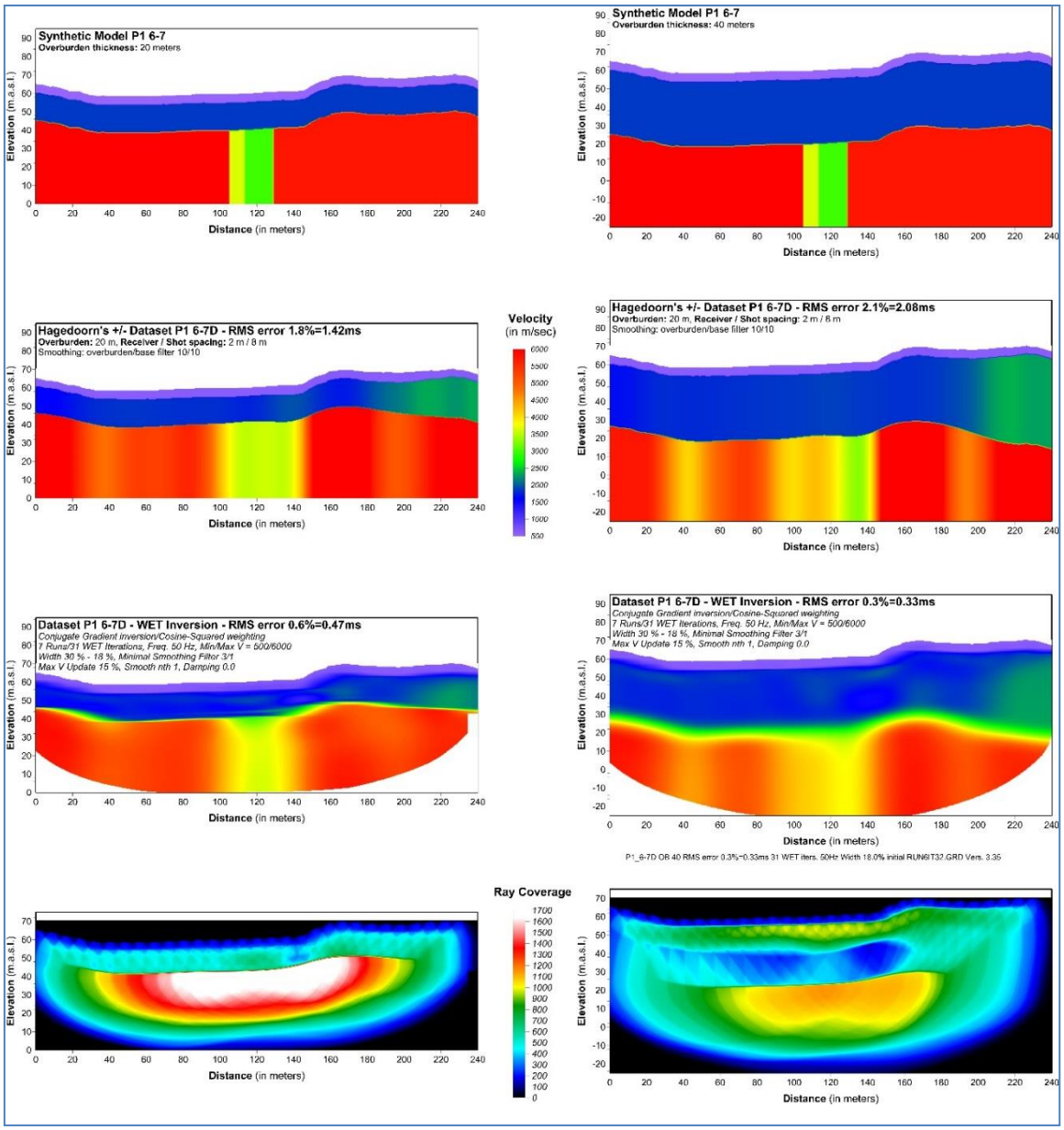

Figure 7.2.1: *P1-6/7 synthetic model (top), Plus-Minus starting model (second), WET Inversion result (third) and Ray Coverage (bottom) for overburden thickness equal to 20 m (left) and 40 m (right).*

Right-hand side **figure 7.2.1** shows the effect of a 40 m overburden layer in model P1-6/7. This time, the Plus-Minus starting model shows a more dubious bedrock fragmentation below the overburden with a large ambiguous low-velocity area and the most pronounced fracture zone displaced to the right compared to the modeled pair. Artefacts that could be interpreted as additional fracture zones can also be seen left and right of the middle part of the profile, but after the application of WET inversion they are suppressed, and more weight is given on the actual modelled zones area. The inversion result is not perfect since it fails to concentrate the ambiguous low-velocity area within the limits of the modeled zones, but at least indicates that there is a low-velocity area that could be interpreted as a fracture zone beneath 40 m of overburden.

The Ray Coverage plot seen at bottom right of **figure 7.2.1**, supports deeper investigation possibilities (80 m) but the ray distribution is not very favorable for detecting the modeled fracture zones. As in bottom right-hand side in **figure 7.1.1**, there is a superficial ray concentration (700-1000 rays) that only covers part of the overburden, followed by an underlying low ray-coverage band (100-300 rays). However, since model P1-6/7 contains more geophones and shot points than P1-1 and offers a higher depth coverage, the ray concentration increases again (1100 rays) exactly at the boundary between overburden and bedrock, resolving a part of the modeled pair of fracture zones. Therefore, it is possible to obtain information with WET inversion on refraction seismic data even with the presence of 40 meters of overburden on top of possible fracture zones. Artificial effects such as gradient change in the velocity, too high central velocity and unclear zone thickness appears in model fracture zone as well as a new possible fractured zone.

8. DISCUSSION AND CONCLUSIONS

Testing the effectiveness of DeltatV method in producing relatively accurate starting models to be used in WET inversion in Rayfract® has only partly been successful. Two synthetic models were tested with a variety of dense receiver/shot point spacing. At our first attempt, all cases revealed that modeled fracture zones are almost impossible to detect with certainty if not at all while the obtained profiles are filled with artefacts.
Contrary to our mainly unsuccessful results, S. Rohdewald's processing effort on the data has shown that DeltatV with enabled XTV option can yield good starting models at least for the case of model P1-6/7. For model P1-1 where DeltatV / XTV application did not yield successful starting models, more elaborate WET inversion schemes have indeed led to the detection of the fracture zones modelled even if the interpretation of their velocity, shape and positioning is dubious. P1-6/7 WET inversion by S. Rohdewald has returned very good results concerning the fracture zone when 1 m geophone spacing was used, but results deteriorated with receivers positioned every 2 m. Positioning and velocity of the modeled zone were accurate with datasets A and B but all results present the zone as an inverted triangle. When datasets C and D are inverted, the zone is underestimated in velocity and shown unified with the basin overlaying it. Regardless, when favorable conditions are present and refraction data are collected densely enough, DeltatV / XTV can provide good starting models for our synthetic data sets but not as good as obtained with Hagedoorn's Plus-Minus method.

The conditions that inhibit the use of DeltatV which were explained in the beginning of chapter 4, are still valid even though the synthetic datasets were constructed with a high receiver/shot point spacing density. However, real refraction seismic surveys in Norway are implemented with much sparser receiver and shot point spacings (5 m and 30 m respectively). Moreover, S. Rohdewald has brought more details to our attention regarding our models which make it difficult for DeltatV to achieve really good results in creating starting models. For example, more offset shots are required at the edges of a 240-m long profile such as P1-6/7 i.e. at 10, 20, 40, 60, 80, 100 and 120 meters at each side whereas our models only contain two offset shots per side (at 60 and 120 m). Closer spaced far-offset shots result in more closely sampled CMP curves at bottom of Midpoint breaks display and thus at bottom of resulting DeltatV inversion output. Furthermore, if the topography undulates extremely along the profile as in our models, then DeltatV combined with XTV has issues "deciding" if lateral delays on traveltime curves are caused by topography or underlying low-velocity variation. This is also due to the fact that no refractor mapping of first breaks is done for DeltatV / XTV. Such rough topography is commonly encountered in Norway and in most cases difficult to smoothen enough for DeltatV / XTV to become as effective as over flat surfaces. Our two synthetic models are based on real seismic interpretation from a tunnel project in Norway.

We have used the knowledge obtained in previous NGU reports about how to run WET inversion on data to detect fracture zones and applied it on these densely constructed synthetic datasets. It was shown that the application of Hagedoorn's Plus-Minus method with interactive picking of branch points can yield starting models which are very close to the synthetic model (Tassis et al. 2017). Subsequent multirun WET inversions do not shift the results much and only add to the success of the method with lower RMS errors for all cases. Due to the nature of the synthetic models i.e. perfect verticality of fracture zones, uniform velocities for each block and no gradual velocity change between different blocks, Hagedoorn's Plus-Minus method results can be preferred over WET inversion results. Using Plus-Minus starting models with branch point picking, all modeled fracture zones are detected in detail both in qualitative and quantitative terms.

Synthetic datasets produced with denser receiver/shot point spacing require less specialized Plus-Minus processing and WET inversion parameters and can give accurate results with almost default Rayfract® settings. Generally, not as densely modeled (or collected) data require lower *Smoothing overburden* and *base filter* values for Plus-Minus to achieve a desired vertical fragmentation in bedrock. Such lateral variations in velocity is required to be able to image fracture zones and subsequently more intense smoothing removal has to be applied so that WET inversion can calculate the characteristics of these zones correctly. The choice of parameters in studies like this is facilitated, steered and perfectioned by the knowledge of the synthetic model. In real life, the creation of a starting model and subsequent inversion are totally up to the intuition of the Rayfract® user, but densely collected data render processing easier and more robust.

Hagedoorn's Plus-Minus method with interactive branch point picking is not the only reliable method for producing a starting model in Rayfract®. Branch point picking itself enables the use of Wavefront method (equivalent to GRM method, Palmer 1980) in addition to Plus-Minus, whereas the user can also use midpoint breaks to avoid the time-consuming procedure of manually mapping traces to refractors using branch

points. The semi-automatic midpoint breaks mapping option also enables using either Plus-Minus or Wavefront method to produce a starting model. It was decided to dedicate some time to investigate this with the help of Rayfract® developer S. Rohdewald. The starting models obtained after applying Wavefront method using branch points and both Wavefront and Plus-Minus methods using midpoint breaks were very good but also showed some weaknesses that Plus-Minus method with branch point picking does not have. Underestimation of zone velocities, top-layer thickness smaller than modeled for dataset P1-6/7A, not seeing a 2200 m/s soil layer at dataset P1-1 and artefacts at the edges of the profiles especially for dataset P1-1A let us conclude that **Hagedoorn's Plus-Minus method with interactive branch point picking is still our best option for producing starting models** for the kind of data we have tested.

Finally, we have investigated the effect an overburden layer of low velocity and various thickness can have on the inversion process and the detection of underlying fracture zones. We used the same models as before with receiver/shot spacing equal to 2/8 meters (dataset D) and added two simple overburden layers to them with thicknesses equal to 20 and 40 m. The most useful conclusions obtained from this investigation were provided by mapping ray coverage after the application of multirun WET inversion. We showed that 20 m of overburden deteriorate both starting model and inversion result quality for both models, but zone detection is still possible. However, 40 m of overburden render the task of accurately unveiling underlying zones almost impossible, especially when shorter receiver arrays are employed. Depth coverage for model P1-1 (120 m length) is close to 50 m while model P1-6/7 (240 m length) presents a ray coverage that reaches a maximum depth of 80 m. The distribution of rays is also of interest since the presence of thick overburden leads to a high ray coverage, and by this good estimate of soil thickness. However, the longer the array is, the deeper we can obtain information from WET inversion. All models were constructed with the use of four distant shots, two per each side of the profile and equal to maximally half the profile's length as suggested by S. Rohdewald. More densely spaced offset shots preferably recorded with overlapping receiver spreads should probably improve the penetration depth.

9. REFERENCES

Hagedoorn, J.G. 1959: The Plus-Minus method of interpreting seismic refraction sections. Geophysical Prospecting 7 (2), pp.158 – 182.

Gebrande, H. & Miller, H. 1985: Refraktionsseismik (in German). In: F. Bender (Editor), Angewandte Geowissenschaften II. Ferdinand Enke, Stuttgart; pp. 226-260. ISBN 3-432-91021- 5.

Golden Software, 2018: Surfer 15, ver. 15.4.354 - Powerful Contouring, Gridding & 3D Surface Mapping Software. Golden Software, LLC, Colorado, USA.

Palmer, D. 1980. The Generalized Reciprocal Method of Seismic Refraction Interpretation. Society of Exploration Geophysicists, Tulsa. ISBN 0-931830-14-1.

Rayfract 2018a: Rayfract Seismic Refraction & Borehole Tomography- Subsurface Seismic Velocity Models for Geotechnical Engineering and Exploration. Downloaded from http://rayfract.com

Rayfract 2018b: Rayfract help. Download from http://rayfract.com/help/rayfract.pdf

Rønning, J.S., Tassis, G., Kirkeby, T. & Wåle, M. 2016: Retolkning av geofysiske data og sammenligning med resultater fra tunneldriving, Ringveg Vest i Bergen. NGU Report 2016.048 (48 pp. in Norwegian).

Schuster, G.T. & Quintus - Bosz, A. 1993: Wavepath Eikonal Traveltime Inversion: Theory. Geophysics vol. 58, pp. 1314 – 1323.

Tassis, G., Rønning, J.S. & Rohdewald, S. 2017: Refraction seismic modelling and inversion for the detection of fracture zones in bedrock with the use of Rayfract® software. NGU Report 2017.025 (62 pp.).

Wåle, M. 2009: Refraksjonsseismiske undersøkelser Ringveg vest, byggetrinn 2 Sandeide-Liavatnet. GeoPhysix, Rapport nr. 09171 (in Norwegian).

GEOLOGICAL
SURVEY OF
NORWAY

· NGU ·

Geological Survey of Norway
PO Box 6315, Sluppen
N-7491 Trondheim, Norway

Visitor address
Leiv Eirikssons vei 39
7040 Trondheim

Tel (+ 47) 73 90 40 00
E-mail ngu@ngu.no
Web www.ngu.no/en-gb/